

University of Trento  
Department of Industrial Engineering



UNIVERSITY  
OF TRENTO

---

Mechanical Design for Mechatronics

## JANSEN'S LINKAGE

**Professor:**

Prof. Emiliano Rustighi

**Group number:**

10

**Students:**

Lorenzo Colturato, 233301

Paolo Furia, 201968

Mahyar Shamsikolokhi, 230898



# Abstract

This project has the aim to present a particular type of planar linkage that can be used for the design of legged mechanisms, the Jansen's linkage. The report starts with an introduction about legged mechanisms and their historical background, which states the most important accomplishments in this field in chronological order, and continues with the design criteria that have to be considered when designing a legged machine, how the Jansen's linkage stands in relation to these criteria, and finally Chapter 1 ends reporting the main applications of the linkage. Chapter 2 presents a general study on linkages and, particularly, on Jansen's linkage. Chapter 3 explains the kinematic analysis of the linkage, therefore the derivation of the position, velocity and acceleration of all the links, while Chapter 4 is about the dynamic analysis, which has the aim to determine the forces and torques in the system. To carry out the kinematic analysis and the dynamic analysis we relied on reference [1], a master thesis about the design and optimization of Theo Jansen's mechanism. Chapter 5 introduces an already existing project based on the use of Jansen's linkages as legs to allow the motion of the mechanism. Finally, the conclusions are shown in Chapter 6.



# Table of Contents

<b>List of Figures</b>	<b>1</b>
<b>List of Tables</b>	<b>1</b>
<b>1 Introduction</b>	<b>3</b>
1.1 Legged mechanisms . . . . .	3
1.1.1 Historical background . . . . .	4
1.2 Design criteria for legged machines . . . . .	7
1.3 Main applications . . . . .	8
1.3.1 Strandbeest . . . . .	8
1.3.2 Other applications . . . . .	9
<b>2 Linkages</b>	<b>11</b>
2.1 Jansen's leg mechanism . . . . .	16
2.1.1 Design parameters for the optimization of link geometry . . . . .	18
<b>3 Kinematic Analysis</b>	<b>20</b>
3.1 First kinematic chain - z1z2z3z4 . . . . .	21
3.2 Second kinematic chain - z1z2z5z6 . . . . .	24
3.3 Third kinematic chain - z6z8z9z10 . . . . .	26
<b>4 Dynamic analysis</b>	<b>28</b>
4.1 Dynamics of link z2 . . . . .	31
4.2 Dynamics of link z3 . . . . .	32
4.3 Dynamics of coupling z4z7z8 . . . . .	33
4.4 Dynamics of link z5 . . . . .	34
4.5 Dynamics of link z6 . . . . .	35
4.6 Dynamics of link z9 . . . . .	36
4.7 Dynamics of coupling z10z11z12 . . . . .	37
<b>5 Design example. Quadruped robot for obstacle avoidance</b>	<b>38</b>
<b>6 Conclusions</b>	<b>43</b>
<b>References</b>	<b>44</b>



# List of Figures

1.1	One of Jansen's Strandbeest. This image is licensed under CC BY-SA . . . . .	8
1.2	Different applications and Jansen mechanism based projects . . . . .	10
2.1	Links of different order [2] . . . . .	11
2.2	Gruebler paradoxes [2] . . . . .	13
2.3	Joint order examples [2] . . . . .	13
2.4	Watt and Stephenson isomers for a sixbar linkage [3] . . . . .	14
2.5	Types of four-bar linkages Cdang, Salix alba is licensed under CC BY-SA 3.0 . . . . .	15
2.6	Jansen's leg mechanism with the parameters regarding the links and the foot trajectory	16
3.1	Jansen's linkage scheme . . . . .	20
3.2	First kinematic chain . . . . .	21
3.3	Second kinematic chain . . . . .	24
3.4	Third kinematic chain . . . . .	26
4.1	Free body diagram of a general binary link . . . . .	29
4.2	Free body diagram of the forces in a general triangular coupler . . . . .	30
4.3	Free body diagram of the link z2 . . . . .	31
4.4	Free body diagram of the link z3 . . . . .	32
4.5	Free Body diagram of the coupling composed by the links z4z7z8 . . . . .	33
4.6	Free body diagram of the link z5 . . . . .	34
4.7	Free body diagram of the link z6 . . . . .	35
4.8	Free body diagram of the link z9 . . . . .	36
4.9	Free Body diagram of the coupling composed by the links z10z11z12 . . . . .	37
5.1	CAD model and trajectory followed by various joints . . . . .	38
5.2	CAD model of the whole machine [4] . . . . .	39
5.3	<i>Simulink</i> models . . . . .	39
5.4	Prototype model of the robot [4] . . . . .	40
5.5	Fuzzy-based obstacle avoidance system [4] . . . . .	40
5.6	Distance of the robot from: the target (left), the obstacle (right) [4] . . . . .	41
5.7	Output function of the controller: angular velocities of the motors [4] . . . . .	41
5.8	Setup for obstacle avoidance validation [4] . . . . .	41
5.9	Results of the obstacle avoidance validation [4] . . . . .	42

# List of Tables

1.1	Timeline table of some walking machines [5][6] . . . . .	6
2.1	Number of possible isomers depending on the number of links . . . . .	14
2.2	Holy numbers from the genetic code . . . . .	17

# Chapter 1

## Introduction

The expansion of using robots in human life is becoming a more attractive area of research and development. This expansion has led many to start advancing automated machinery aimed at different applications. Over the past decades the development of science and technology improved the design and production of robots from fiction to reality. Different applications within different disciplines such as computer science, medical application, fields of engineering and automation played a great role in the advancements within robotics. A locomotion over a soft or hard surface by means of limbs, legs and/or wheels can be defined as a walking machine. The design and development of these machines have been widely studied by researchers and companies like NASA where the application involves manoeuvrability over rough terrains and planetary exploration since the 1960s. Nowadays three basic types of walking machines can be found: wheeled, tracked and legged walking machines (or robots) [7]. Legged robots have always been a favourite for researchers but also the most complicated solution where the application involves manoeuvrability over rough terrains. This research field has attracted great interests in the past decades and a lot of prototypes have been successfully built in the university laboratories or companies.

### 1.1 Legged mechanisms

By definition a leg mechanism (walking mechanism) is a mechanical system designed to provide a propulsive force by particular intermittent frictional contact with the ground. This is in contrast with wheels or continuous tracks which are intended to maintain continuous frictional contact with the ground. Mechanical legs are linkages that can have one or more actuators, and can perform simple planar or complex motion. Compared to a wheel, a leg mechanism is potentially better fitted to uneven terrain, as it can step over obstacles. The path of the motion of the leg can be modified depending on the terrain that the robot will go on.[8]

The main advantages of walking machines over wheels are:[9]

1. Contact with the ground at discrete points
2. Elimination of roads
3. Minimal contact area with the ground
4. Reduced ground pressure

5. Machine height
6. Increased traction
7. Potential application as an amphibian
8. Climbing abilities

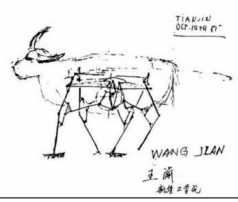
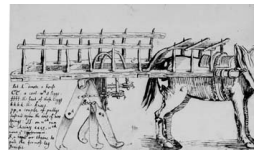
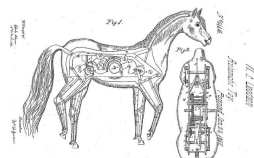
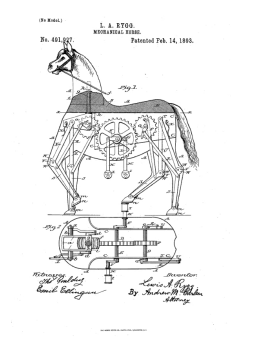
The main disadvantages of walking machines over wheels are:[9]

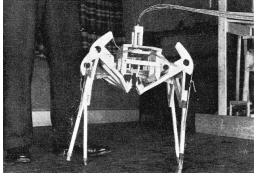
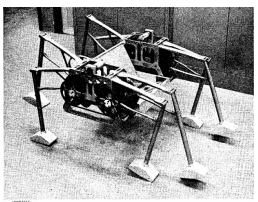
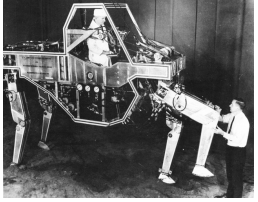
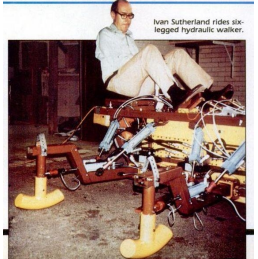
1. Energy inefficiency
2. Complicated to design
3. Costs
4. Novelty

The earliest walking machines were mechanical toys. Their legs were driven by cranks or cams from a source of rotary power, usually clockwork, and executed a fixed cycle. The main event which led to the consideration of practical walking machines was the invention of the internal combustion engine, which made possible all sorts of new vehicles. One line of development consisted of extending wheels and caterpillar tracks by attaching feet, spikes or posts to the rim or to sections of the track.[6]

### **1.1.1 Historical background**

Table 1.1 lists the most important walking machines (and ideas) in chronological order, starting from the third century BC with the realization of wooden oxen as transport vehicles and similar rural machines, arriving at the turn of the 90s of the 20th century when the Jansen's leg mechanism was made.

Year	Maker	Country	Description	Image
230 BC	Zhu-ge Liang	China	<b>Wooden Oxen</b> and Gliding Horse - Born as a transport vehicle	
1663	Potter/ Hooke	UK	<b>Cart with Legs</b> - Presented to the Royal Society	
1850	Chebyshev	Russia	<b>Chebyshev Walking platform</b> - Four bar mechanism that converts rotational motion to approximate straight-line motion with approximate constant velocity. The Chebyshev's Lambda Mechanism is a cognate linkage of the Chebyshev linkage and is still used in vehicle suspension mechanisms, walking robots and rover wheel mechanisms	
1867	W. Farr Goodwin	USA	<b>Mechanical Horse</b> - Patented in 1867	
1892	L. A. Rygg	USA	<b>Mechanical Horse</b> - Patented in the USA in 1893 but no prototype was ever built	

1940	Hutchinson and Smith	UK	<b>Walking SuperTank</b> - The first military related walking machine with independently controlled legs. The proposed control mechanism consisted of a feedback loop per leg, with the four legs each being controlled by the hand or foot of the drive	
1968	R. A. Morrison	USA	<b>Iron Mule Train</b> - Only one carriage was built for test purposes	 Figure 2. Walking Mechanism Assembly
1969	General Electric, Ralph Mosher	USA	<b>Walking Truck</b> - GE to turn-out a semi-amphibious four-legged, cargo-carrying CAM (Cybernetic Anthropomorphic Machine). The complex movements of the legs and body pose were done entirely through hydraulics	
1976	McGhee	USA	<b>OSU Hexapod</b> (Probably derived from "Phony Pony" developed at the University of Southern California (USC)) - It is the first legged machine whose walking cycle was generated by a digital electronic controller	 Figure 1. OSU Hexapod Vehicle showing ability to maintain body level while crossing rough terrain
1983	Ivan Sutherland	USA	<b>Six-Legged Hydraulic Walker</b> - The robot used a gasoline motor to power its legs and required a driver to operate it via foot pedals. The machine would keep three legs on the ground at any given time, eliminating the need for balancing systems, though also limiting the speed of the system. Each leg could move forward, backwards, and side-to-side, allowing it to navigate across uneven surfaces	 Ivan Sutherland rides six-legged hydraulic walker.
1990	Theo Jansen	The Netherlands	<b>Strandbeest</b> - Never patented kinetic sculpture made of multiple legs also called Jansen's linkages	

**Table 1.1:** Timeline table of some walking machines [5][6]

## 1.2 Design criteria for legged machines

When designing a walking machine the following design criteria are to be taken into consideration:[9]

- Static balance. The mechanism should not require a balance control system and therefore should remain in balance on its own
- Minimal power consumption
- Minimum number of prime movers. The mechanism should have the minimum number of movers to allow movement and to facilitate manufacturing and maintenance
- The prime mover should preferably require rotary rather than linear motion. Rotary movers are easier to carry and require simpler systems
- Deterministic foot trajectory. The mechanism should not need control systems and ground sensing
- A slow return mechanism. A slow return mechanism is needed in order to reduce dynamic loads in the leg's return movement
- A stiff mechanism. A stiff mechanism is required to make sure that the movement of the body is controlled by the movement of the legs
- Hinged legs. Hinged legs are necessary to control the position of the body to keep it in the same horizontal plane minimizing variation in potential energy
- A scalable design. A scalable design is helpful because in this way it is possible to make a smaller prototype with respect to the full sized mechanism that permits to simplify the testing and validation phases
- The final design should be for a large walking machine. A large walking machine allows to carry heavy loads and tons of material

With respect to the design criteria stated before it can be said that Jansen's linkage represents a valid mechanism for use as a leg for a walking machine. [9] A six or eight legged mechanism which makes use of Jansen's legs should allow static balance, while quadruped machines are less efficient. As Jansen's linkage features a single actuator the power consumption is low. The "Strandbeest", a structure made up of Jansen's linkages which will be explored in the next paragraph, is composed of a single crankshaft to move all the legs and this leads to longitudinal movements between the feet, so they cannot remain firmly planted on the ground. [9] Therefore, to avoid this type of problem a two crankshaft mechanism should be implemented where the two crankshaft have to be driven together. The necessary power to move the leg is provided by a crank which rotates actuated by a motor. Since all the components of the mechanism moves with respect to the actuated crank there is only one DOF, therefore the foot position is deterministic because it can be found knowing the link dimensions and the position of the crank. With a careful design concept the Jansen mechanism can be made to have a gentle foot return trajectory, so the dynamic loads are reduced. [9] Generally, this type of mechanism is realized with stiff links so, in order for the mechanism to be stiff enough,

the crankshaft should not experience large displacements and should remain in position. The leg joint is typically hinged so potential energy's variation are not a problem. Finally, being a planar mechanism, Jansen's linkage is easily scalable so it can be scaled down to simplify the testing phase and then realized as a full size for the final usage.

### 1.3 Main applications

For all of the reasons stated in Section 1.2 Jansen's mechanism is suitable for lots of applications regarding walking machines. Theo Jansen's work, the Strandbeest, has already been introduced as the main work of the Dutch artist. Despite its size and prominence the Strandbeest was intended as a kinetic sculpture, so it does not have many practical applications. The most important application of the Jansen's linkage is walking motion used in legged robotics mainly for its scalable design, minimum power consumption, deterministic foot trajectory etc. In this way it is possible to realize legged robots capable to deal with complex obstacles, rapid change of direction, mobility on rough terrains and high manoeuvrability. Some example of Jansen's leg mechanism applications are given below, starting with the Strandbeest.

#### 1.3.1 Strandbeest

Since 1990 Theo Jansen has been creating kinetic sculptures which he has constantly improved over the years, arriving in 2007 with the creation of the Strandbeest, which means "beach animal" in Dutch. Every year Theo Jansen brings one or two new sculptures to the Dutch beaches, so the Strandbeest is constantly evolving. In fact there are many different types of Strandbeest that differ mainly in size, shape and way of moving. The overall idea is to recreate animals' way of moving with a mechanism which ultimately survives on its own. In Figure 1.1 one of Theo Jansen's Strandbeest can be seen.



**Figure 1.1:** One of Jansen's Strandbeest. This image is licensed under CC BY-SA

This type of Strandbeest is a mechanism made up of Jansen's linkages and, as can be seen in Figure

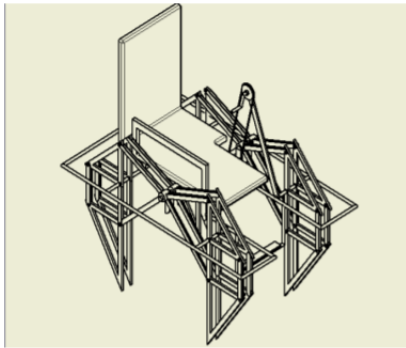
1.1, it is powered by wind using sails, allowing the structure to roam the shores of the Netherlands beaches. The construction is based on non-biological objects such as PVC plastic pipes and wood, to reduce the weight of the mechanism and production costs and to promote fluid movement, held together by strings.[10] In this way Theo Jansen created a planar mechanism (which is the leg) that, when used in tandem with many others identical to it, can walk in a smooth forward motion by harnessing the power of the wind.[11] In combination with the action of the wind there are also some air tubes that act like pistons, which are connected with the wings (the sails part), that pump air to high pressure into empty bottles made of plastic and this enables the mechanism to have still a little bit of energy to allow its movement when the wind falls away.

As said before, the Strandbeest can be useful as a transportation vehicle, but from the beginning it was intended just as a kinetic sculpture with no practical use. For this reason Theo Jansen has created a website ([12]) where he explains how his mechanism work and the genealogy and future evolutions of the Strandbeest, so everyone can study it and find a way to implement this legged mechanism for more useful applications. Several people developed legged machines based on Theo Jansen's works and in the next paragraph some of these projects will be presented.

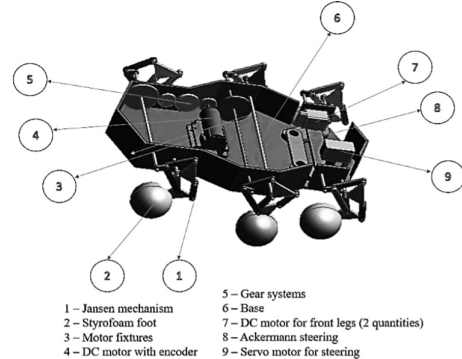
### 1.3.2 Other applications

In the last years Theo Jansen's works have become so popular that many curious people have decided to start developing machines based on Jansen's leg mechanism. In fact, he decided never to patent his idea to allow everyone to use his mechanism as a basis to create something other than Strandbeest, which could have other purposes and applications. Several projects have been carried out, mainly involving university students and researchers, who starting from the Jansen's mechanism have created legged machines that can have applications in robotics, such as walking mobile robots, and can be used to develop robots for exploration and surveillance tasks, systems that can walk on both ground and water surfaces, rough terrains and robot for obstacle avoidance or gait analysis. In 2015 the *International Journal of Engineering Research & Technology (IJERT)* published an article that presented a walking chair using Jansen's linkages with the intention of exploiting the advantages of the walking motion over the traditional rolling motion to help people with locomotive disability.[13] This machine could be useful especially in poor Countries like India where most of the disabled population resides in the rural areas and don't have the money to afford wheelchairs. In 2016 *Springer Singapore* published a design work of an amphibian legged robot based on Jansen mechanism that can walk on both ground and water surfaces and can be used for exploration and surveillance tasks. In fact, all previous machines were meant to walk only on the ground while this system opens the way for a linkage based robot to walk on water surfaces. To accomplish that the Jansen legged mechanism has been redesigned in order to improve the drag force during walking on the water surfaces.[14] In 2019 a team of students from China designed a hexapod robot based on non-collocated actuators to implement a distributed control system for the locomotion of the robot. In this way the robot uses only three motors while most of existing hexapod robot with collocated actuators require 18 servos. This allow the robot to be much cheaper than the traditional ones.[15] In 2020 was published by the *Arabian Journal for Science and Engineering* an article about the development of a Jansen mechanism-based quadruped robot that exploits the advantages of the wheel mobile robots for use over uneven terrains and for obstacle avoidance.[4] In Figure 1.2 four design projects based on the use of Jansen's linkage can be seen (those reported

previously), respectively the walking chair in 1.2a, the amphibian legged robot in 1.2b, the hexapod legged robot in 1.2c and finally the quadruped robot in 1.2d.



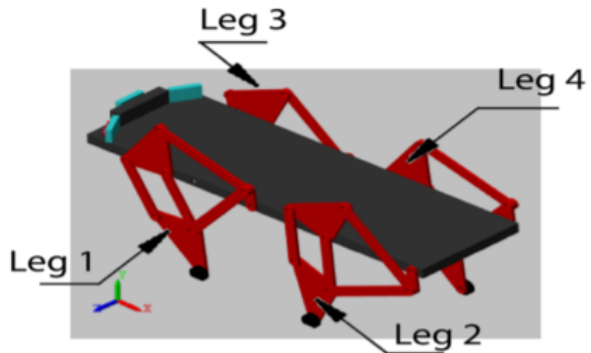
(a) Walking chair [13]



(b) Amphibian legged robot [14]



(c) Hexapod robot [15]



(d) Quadruped robot for obstacle avoidance [4]

**Figure 1.2:** Different applications and Jansen mechanism based projects

Particularly, in Chapter 5 the quadruped robot for obstacle avoidance is studied and analyzed more deeply.

# Chapter 2

## Linkages

Linkages are the basic building blocks of all mechanisms and are made up of links connected at joints by different type of fasteners, usually rotary or linear bearings. A link, as shown in Figure 2.1, is a rigid body that possesses at least two nodes, which are points for attachment to other links. They are classified in binary links, ternary links and quaternary links, depending on the number of connection points (nodes) they have.

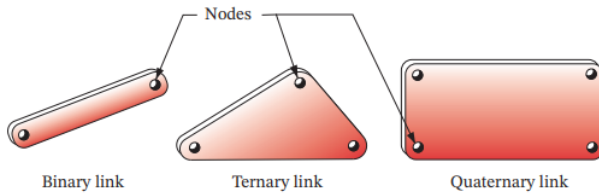


**Figure 2.1:** Links of different order [2]

A joint, also called kinematic pair, is a connection between two or more links at their nodes, which allows some relative motion between the connected links. They can be classified by:

- the type of contact between the elements
- the number of Degrees of Freedom (DoF) allowed at the joint
- the type of physical closure of the joint: either force or form-closed
- the number of links joined (order of the joint)

Franz Reuleaux coined the term "lower pair" to describe joints with surface contact (as with a pin surrounded by a hole) and the term "higher pair" to describe joints with point or line contact. The main practical advantage of lower pairs over higher pairs is their better ability to trap lubricant between their enveloping surfaces, thus reducing friction phenomena. Among the lower pairs figure single DoF joints such as the revolute, the prismatic and the helical, and multiple Dof joints such as the cylindrical, the spherical and the planar. The revolute (R) and the prismatic (P) pairs are the only lower pairs usable in a planar mechanism and, while the revolute joints only allow the rotational motion between members, the prismatic joint, also called sliding joint, allows the linear translational motion. The helical (H), cylindrical (C), spherical (S), and planar (F) lower pairs are

all combinations of the revolute and/or prismatic pairs and are used in spatial (3-D) mechanisms. Particularly, the cylindrical and the helical are the superposition of a revolute and a prismatic joints, but if the cylindrical is a 2 DoF lower pair joint, the helical has only one DoF. The spherical and the planar, instead, are a combination of three revolute joints and both of them are three DoF multiple joints. The concept of degrees of freedom is fundamental to both the synthesis and analysis of mechanisms. Degrees of freedom (also called mobility ( $M$ ) of a system) can be defined as the number of inputs that need to be provided in order to create a predictable output, or the number of independent coordinates required to define the position of the system.

Kinematic chains or mechanisms may be either open or closed. A closed mechanism will have no open attachment points or nodes and may have one or more degrees of freedom. An open mechanism of more than one link will always have more than one degree of freedom, like an industrial robot. The DOF of a planar linkage mechanism can be predicted from the Gruebler's equation:

$$M = 3(L - 1) - 2J \quad (2.1)$$

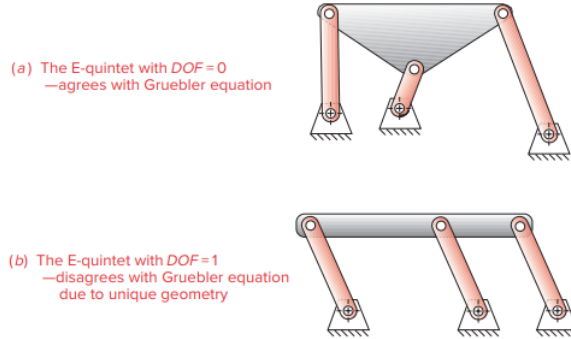
where  $M$  is the degree of freedom or mobility,  $L$  is the number of links and  $J$  the number of joints. Sometimes it is less confusing using the Kutzbach's modification of Gruebler's equation in this form:

$$M = 3(L - 1) - 2J_1 - J_2 \quad (2.2)$$

where in this case  $J_1$  is the number of 1 DOF (full) joints and  $J_2$  is the number of 2 DOF (half) joints. The half joint is also called a roll-slide joint because it allows both rolling and sliding and, considering equation 2.1, we have to consider  $J=\frac{1}{2}$ . Equation 2.2 can be used for planar mechanisms, therefore for spatial mechanisms it can be reformulated in the following formula:

$$M = 6(L - 1) - 5J_1 - 4J_2 - 3J_3 - 2J_4 - J_5 \quad (2.3)$$

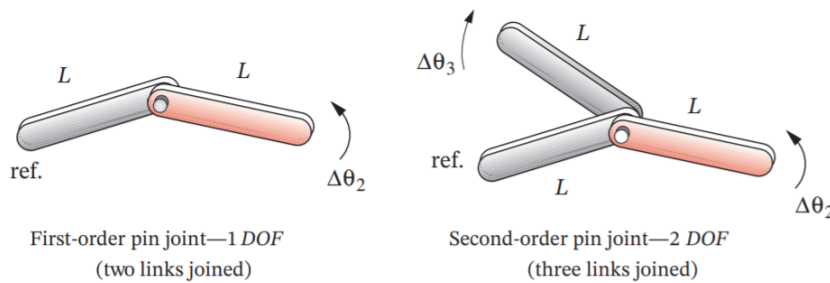
The mobility predicts the type of the mechanism. There are only three possibilities: if the DoF is positive, it will be a mechanism, and the links will have relative motion; if the DoF is exactly zero, then it will be a structure, and no motion is possible; otherwise, if the DoF is negative, it is a preloaded structure, which means that no motion is possible and some stresses may also be present at the time of assembly. Because the Gruebler's criterion pays no attention to link sizes or shapes, it can give misleading results in the face of unique geometric configurations. Referring to Figure 2.2, the first image shows a structure ( $DoF = 0$ ) that behave as predicted in Gruebler's equation with the ternary links of arbitrary shape. The second image is the same but with the ternary links straight and parallel of equal length and with equispaced nodes. It can be seen that it will move despite Gruebler's prediction to the contrary.

**Figure 2.2:** Gruebler paradoxes [2]

There are lots of examples of configurations that disobey the Gruebler's criterion due to their unique geometry. For this reason the designer needs to be alert to these possible inconsistencies.

As for the type of the physical closure of the joint, there may be form-closed or force-closed joints. A form-closed joint is kept together by its geometry. A pin in a hole or a slider in a two-sided slot is form closed. Instead, a force-closed joint, such as a pin in a half-bearing or a slider on a surface, needs an external force to keep it together. There are different ways to provide for this force, such as gravity, a spring, or any external means. The choice between form-closed or force-closed joints to use should be carefully considered because there can be substantial differences in the behavior of the mechanism. In linkages, form closure is usually preferred, and it is easy to accomplish. But for cam-follower systems, force closure is often preferred.

Finally, the joint order is defined as the number of links joined minus one, infact it takes two links to make a single joint. The simplest joint combination of two links has joint order one. As additional links are placed on the same joint, the joint order is increased on a one-for-one basis as can be seen in Figure 2.3. Joint order has significance in the proper determination of overall degree of freedom for the system.

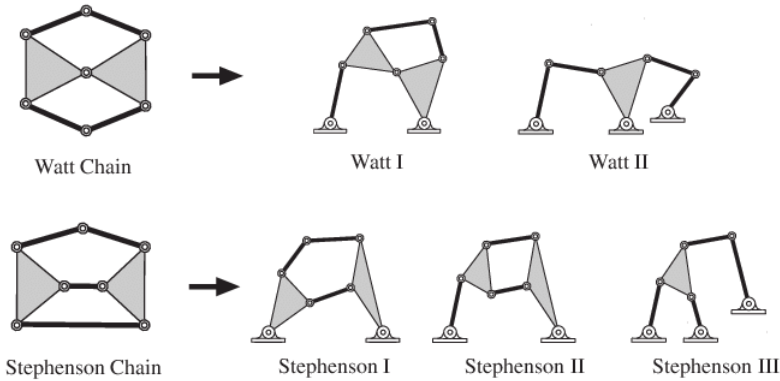
**Figure 2.3:** Joint order examples [2]

Linkages that have the same number and type of links, although interconnected differently, can be called isomers. The links have various nodes available to connect to other links' nodes. Depending on the connections available links, the assembly will have different motion properties. An isomer is only unique if the interconnections between its types of links are different. Depending on the number of connections it is therefore possible to obtain a certain number of isomers as can be seen from Table 2.1.

Links	Possible Isomers
4	1
6	2
8	16
10	230
12	6856

**Table 2.1:** Number of possible isomers depending on the number of links

The 6 link case of 4 binaries and 2 ternaries has only two valid isomers: Watt's chain and Stephenson's chain, which are reported in Figure 2.4.

**Figure 2.4:** Watt and Stephenson isomers for a sixbar linkage [3]

The four-bar linkage composed by four binary links and four revolute joints is the simplest possible pin-jointed mechanism for single DoF controlled motion. It is commonly used for moving platforms, clamping, and for actuating buckets on construction equipment, indeed it is very versatile in terms of the types of motion that it can generate. The Grashof condition is the relationship that predicts the rotation behaviour of a four-bar linkage's inversions based only on the link lengths.

$$S + L \leq P + Q \quad (2.4)$$

where  $S$  is the length of the shortest link,  $L$  is the length of the longest link,  $P$  is the length of one remaining link and  $Q$  is the length of the other remaining link. If is true, then the linkage is Grashof and at least one link will be capable of making a full revolution with respect to the ground plane. There are three possible cases:

- Class I case:  $S + L < P + Q \Rightarrow$  the mechanism exist and it could be a crank-rocker, double-crank, rocker-crank or double-rocker
- Class II case:  $S + L > P + Q \Rightarrow$  not a Grashof mechanism; no link can fully rotate
- Class III case:  $S + L = P + Q \Rightarrow$  the mechanism exists and could be double-cranks or crank-rockers but will have “change points” conditions twice per revolution of the input crank when the links all become collinear, condition for which the behavior of the linkage becomes unpredictable because it can assume either of two configurations

For the first case, grounding either link adjacent to the shortest we get a crank-rocker, in which the shortest link will fully rotate and the other link pivoted to ground will oscillate; grounding the shortest link we will get a double-crank, in which both links pivoted to ground make complete revolutions as does the coupler; grounding the link opposite the shortest we will get a double-rocker, in which both links pivoted to ground oscillate and only the coupler makes a full revolution. The third case is also called special case and includes the parallelogram configuration, which is a double-crank and is quite useful as it exactly duplicates the rotary motion of the driver crank at the driven crank. It is often used for industrial robots.

Figure 2.5 portrays the three cases of four-bar linkages previously introduced: drag-link, where both links can do a full revolution, crank-rocker, double-rocker and the parallelogram linkage.

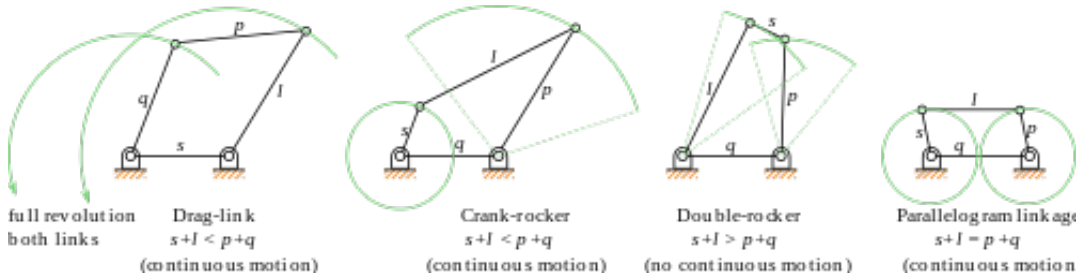


**Figure 2.5:** Types of four-bar linkages  
Cdang, Salix alba is licensed under CC BY-SA 3.0

Beyond the four-bar linkage, which is the simplest one-DoF linkage that can be used for many quite complex motion control problems, there are also five-bar, six-bar linkages and so on for problems where a more complicated solution is necessary. Generally, adding one link and one joint to form a five-bar, the number of DoF will increase by one, to two. Among the six-bar mechanisms there are Watt's and Stephenson's chains, already introduced in Figure 2.4, which can be thought as the assembly of two four-bar linkages connected in series as regards Watt's chain, and in parallel for Stephenson's chain, both of them sharing two links in common. The Grashof's criterion can be readjusted for all single-loop linkages of N-bars connected with revolute joints with the development of a general theorem for linkage rotatability, which returns the following three cases:

- Class I case:  $L_N + (L_1 + L_2 + \dots + L_{N-3}) < L_{N-2} + L_{N-1}$
- Class II case:  $L_N + (L_1 + L_2 + \dots + L_{N-3}) > L_{N-2} + L_{N-1}$
- Class III case:  $L_N + (L_1 + L_2 + \dots + L_{N-3}) = L_{N-2} + L_{N-1}$

where the links are denoted by  $L_i (i=1,2,\dots,N)$ , with  $L_1 \leq L_2 \leq \dots \leq L_N$ .

There is another theorem for the revolvability of any links  $L_i$ , which is defined as the ability of the links to rotate fully with respect to the other links in the chain.

$$L_i + L_N \leq \sum_{k=1, k \neq i}^{N-1} L_k \quad (2.5)$$

It can also be said that if  $L_i$  is a revolvable link, any link that isn't longer than  $L_i$  will also be revolvable.

## 2.1 Jansen's leg mechanism

Theo Jansen realized most of his Strandbeest sculptures, like the one portrayed in Figure 1.1, using several eleven-bar mechanisms that represent the legs of the machine. The linkage is a planar leg mechanism composed of a crank that is actuated by a rotary actuator, for example an electric motor, and moving in a circle it controls the movement of the other links and joints that are unactuated, converting the rotary motion of the crank in a stepping motion. In this way the position and orientation of all the links and joints are determined by the angle of the driving crank, hence the mechanism has only 1 DoF. Jansen's linkage is particularly interesting for robotics applications where chain links are mainly of two types: open chain and closed chain. This linkage is formed by a closed chain where the link, at which the chain terminates, does not have multiple degrees of freedom and is restricted to repeat the same motion throughout its life.[17] In order to create a robot capable to move independently, there is the need to use at least three linkages attached to a motor.

In Figure 2.6a is represented the Jansen's leg mechanism with the parameters that represent the lengths of the links that compose the mechanism.

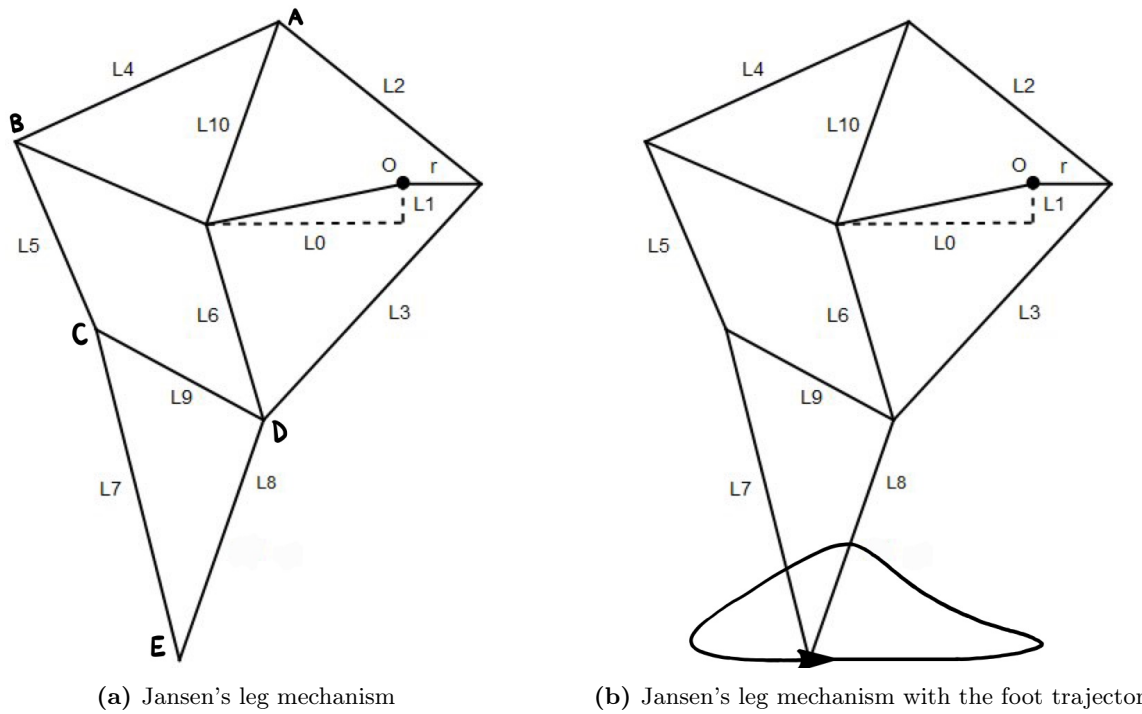


**Figure 2.6:** Jansen's leg mechanism with the parameters regarding the links and the foot trajectory

The parameter "r" is the length of the driving crank which can rotate around the pivot point O, while all the other parameters are the lengths of the remaining links that compose the mechanism. When two Jansen linkages are connected to each other by a rotating horizontal shaft, both the legs help the machine to move forward or backward depending on the clockwise or anticlockwise rotation of the shaft.[17]

After thinking about how to make the leg, in the shape of that of Figure 2.6a, Theo Jansen remained to find the optimal configuration of lengths of the links that have the desired foot trajectory, which can be seen in Figure 2.6b. To find the geometric combination which allows to have the desired

foot trajectory Theo Jansen implemented a genetic algorithm with an initial base of 1500 different combinations of lengths generated from the algorithm itself. The algorithm then evaluated all the combinations and chose the best one hundred, and then recombined them in order to generate another 1500 combinations and so on. The process of elaboration was done on a computer day and night for several months until it returned a result, the so called "genetic code", which provides the "holy numbers", the ultimate combination of lengths of the links that ensure the desired foot trajectory of the leg.

The holy numbers, based on the parameters chosen in Figure 2.6, can be found in Table 2.2.

Parameter	Relative number
r	15
l0	38
l1	7.8
l2	50
l3	61.9
l4	55.8
l5	39.4
l6	39.5
l7	65.7
l8	49
l9	36.7
l10	41.5
l11	40.1

**Table 2.2:** Holy numbers from the genetic code

Using these numbers to design the links of the mechanism Theo Jansen was able to obtain a legged machine that could ensure a smooth movement imitating the way animals move. This is probably the most important advantage of his machines which, however, lack flexibility. In fact, it is impossible to change the foot trajectory without any change of link lengths.[18] One of the main disadvantages of the Jansen's leg mechanism is that the machine walk forward regardless of any obstacle that could be encountered, which are therefore difficult to overcome. A possible solution to this kind of problem was explained in the article [18] where, starting from the conventional Jansen linkage of Figure 2.6, was provided a climbing elliptic orbit by adding another cyclic motion of the central linkage. In this way it is possible, by implementing an appropriate control method, to change systematically the shape of the additional cycle and thus to give the mechanism the capability to walk better on irregular grounds.

As said at the beginning of this Section, the mechanism has eleven bars, which are the links, that are connected through joints which can be assimilated to revolute joints, infact they allow only the rotation of the links following the motion of the actuated crank. Revolute joints are particularly useful because they are relatively easy and inexpensive to design, they build a good quality pin joint, they can be made in such a way, using sleeve or journal bearing, as to have a hydrodynamic lubrication condition, where the parts are separated by a thin film of lubricant to greatly reduce friction problems, and to accomodate the seals to prevent loss of lubricant.

### 2.1.1 Design parameters for the optimization of link geometry

The linkage is represented by the length of its links. By changing the lengths, the trajectory of the foot also varies, thus changing the behavior of the mechanism. There are infinite combinations of link lengths that are achievable, but not all of them have meanings for the design of legged machines because they do not allow to obtain interesting trajectories at practical levels. The following are the main parameters that determine the design of a good legged machine.

#### Duty cycle

The duty cycle of a legged machine is defined as the ratio of the time in which the leg is touching the ground ( $T_1$ ) with respect to the total leg cycle time ( $T_t$ ).

$$DC = \frac{T_1}{T_t} \quad (2.6)$$

The optimal value of DC would be 75%, which allow the design of a statically balanced quadruped machine layout, but this value is difficult to obtain, so a duty cycle about 50% is usually accepted.

#### Mechanism size

Generally, smaller mechanisms are preferred over larger ones for a given performance because they are lighter, have stiffer links and lower inertial loads. The size of the machine can be represented by the sum of the length of the links.

$$L_t = \sum_{i=1}^{10} L_i \quad (2.7)$$

where  $L_t$  is the total link length.

#### Mechanism compactness

The trajectories of the farthest nodes of the linkage will determine how much space, in terms of area, a particular mechanism will need to operate within. Some arrangements need a larger space than others, which will in turn affect the detail design of any walking machine based on this leg proportion. Compactness is defined as

$$A = \frac{x_{C,\min} + x_{O,\max}}{2} \cdot \frac{y_{A,\min} + y_{E,\max}}{2} \quad (2.8)$$

where  $x_{C,\min}$  is the minimum x-value of the trajectory of node C,  $x_{O,\max}$  is the maximum x-value of the trajectory of node O,  $y_{A,\min}$  is the minimum y-value of the trajectory of node A and  $y_{E,\max}$  is the maximum y-value of the trajectory of node E.

#### Stride length

The speed at which a machine is able to move for a given motor speed depends on the stride length of the mechanism, which is given by

$$S_1 = x_{E,\text{fl}} - x_{E,\text{ff}} \quad (2.9)$$

where  $x_{E,fl}$  is the x-value of the trajectory of node E at foot lift, at the end of the stride, and  $x_{E,ff}$  is the x-value of the trajectory of node E at foot fall, at the start of the stride.

### Average speed

Maximum average foot speed corresponds to maximum stride length, in that longer strides will have higher average foot speeds.

$$V_{\text{average}} = \frac{\sum_{i=ff}^{fl} (x_{i+1} - x_i)}{N_w \cdot t} \quad (2.10)$$

where ff is the driving crank index at foot fall and fl at foot lift,  $x_i$  and  $x_{i+1}$  are the position of the foot at instant i and  $i + 1$  respectively,  $N_w$  is the number of time intervals during the walking cycle and t is the time needed for the driving crank to make one revolution.

### Speed fluctuation

The fluctuations in speed determine the smoothness of the walking action of the mechanism and can be quantified by the foot speed fluctuation factor, which is to be minimized.

$$V_f = \frac{\sum_{i=ff}^{fl} (V_i - V_{\text{average}})^2}{N_w} \quad (2.11)$$

where  $V_i$  is the foot velocity at instant i.

### Foot lift

The more the foot of the mechanism, in the return stroke, is able to detach itself from the ground, the more the mechanism has the ability to overcome any obstacles. On the other hand, this requires more energy and results in a longer foot path, so faster foot movement is required.  $h_p$  is the height reached by the foot (point E) with respect to the ground.

$$h_p = y_{E,\text{max}} - y_{E,\text{min}} \quad (2.12)$$

where  $y_{E,\text{min}}$  is the minimum y-value of the trajectory of node E

### Body lift

It can be shown that the amount of vertical movement the body of the mechanism can undergo depends on the trajectory of the foot point when in contact with the ground.[9] Minimizing the body lift ( $L_b$ ) makes the mechanism smoother and more energy efficient.

$$L_b = y_{E,w\text{max}} - y_{E,w\text{min}} \quad (2.13)$$

where  $y_{E,w\text{max}}$  and  $y_{E,w\text{min}}$  are respectively the maximum y-value of the trajectory of node E and the minimum y-value of the trajectory of node E during the walk.

# Chapter 3

## Kinematic Analysis

The kinematic analysis is necessary to know how the mechanism move and to find the position, the velocity and the acceleration of all the links and the joints that compose the mechanism. With the knowledge of these parameters the dynamic analysis can also be performed. In Figure 3.1 a scheme of the Jansen's mechanism can be seen, with all the parameters that are needed to conduct the kinematic analysis.

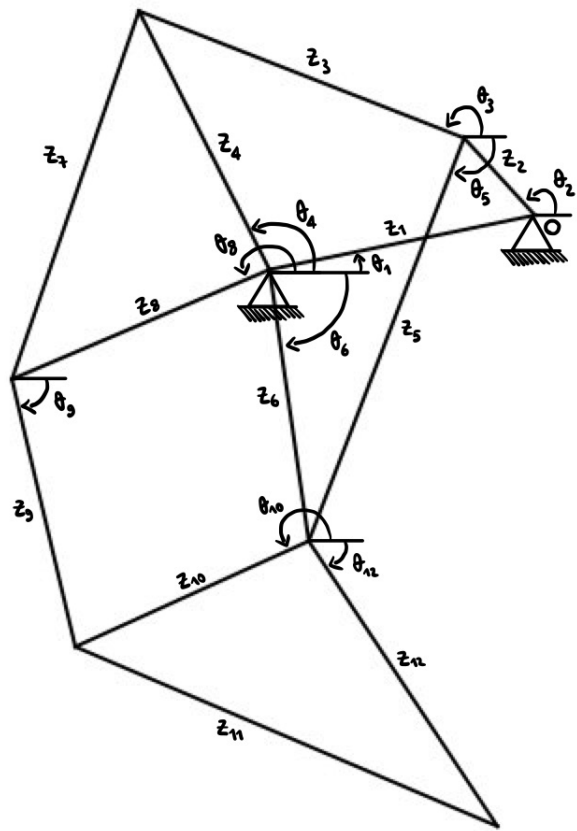


**Figure 3.1:** Jansen's linkage scheme

As said before, the mechanism is controlled only by the driving crank angle, which is  $\theta_2$ , and therefore is a machine with only one DOF to which all the other parameters to calculate them

can be traced. To perform the analysis the mechanism has been broken down into three separate kinematic chains ( $z_1z_2z_3z_4$ ,  $z_1z_2z_5z_6$  and  $z_6z_8z_9z_{10}$ ) that are studied separately writing the chain closure equations for each of the three using the complex numbers method. It should be noted that the angles are positive in the counter clockwise direction and that the driving crank moves with constant angular velocity.

### 3.1 First kinematic chain - $z_1z_2z_3z_4$

In Figure 3.2 is represented the first kinematic chain of the mechanism that is to be studied.

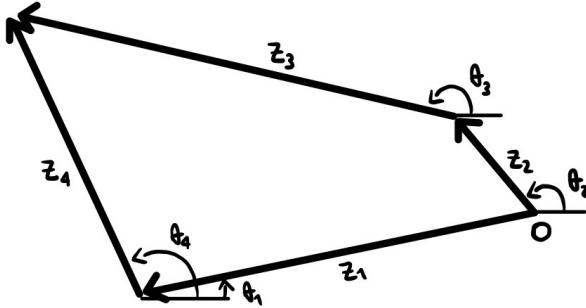


**Figure 3.2:** First kinematic chain

First it is conducted the angular position analysis, then the angular velocity analysis and finally the angular acceleration analysis.

#### Angular position analysis

Below is reported the chain closure equation of the loop  $z_1z_2z_3z_4$ :

$$z_1e^{i\theta_1} + z_4e^{i\theta_4} = z_2e^{i\theta_2} + z_3e^{i\theta_3} \quad (3.1)$$

The closure equation is separated into its real and imaginary parts:

$$\begin{cases} z_1 \cos(\theta_1) + z_4 \cos(\theta_4) = z_2 \cos(\theta_2) + z_3 \cos(\theta_3) & Real \\ z_1 \sin(\theta_1) + z_4 \sin(\theta_4) = z_2 \sin(\theta_2) + z_3 \sin(\theta_3) & Imaginary \end{cases} \quad (3.2)$$

Putting  $C = z_2 \cos(\theta_2) - z_1 \cos(\theta_1)$  and  $D = z_2 \sin(\theta_2) - z_1 \sin(\theta_1)$  and rearranging the equations 3.2 we obtain:

$$\begin{cases} z_4 \cos(\theta_4) = C + z_3 \cos(\theta_3) & Real \\ z_4 \sin(\theta_4) = D + z_3 \sin(\theta_3) & Imaginary \end{cases} \quad (3.3)$$

Squaring the two equations 3.3, adding them together and remembering the fundamental identity of trigonometry ( $\cos^2(x) + \sin^2(x)$ ), we obtain:

$$z_4^2 = C^2 + 2Cz_3 \cos(\theta_3) + D^2 + 2Dz_3 \sin(\theta_3) + z_3^2 \quad (3.4)$$

Putting  $E = C^2 + D^2 + z3^2 - z4^2$  we obtain:

$$2Cz3 \cos(\theta3) + 2Dz3 \sin(\theta3) + E = 0 \quad (3.5)$$

From the fundamental identity of trigonometry,  $\cos^2(\theta3)$  can be substituted with  $\sqrt{1 - \sin^2(\theta3)}$ . At this point rearranging the equation and squaring its members we obtain:

$$4C^2z3^2(1 - \sin^2(\theta3)) = 4D^2z3^2 \sin^2(\theta3) + 4EDz3 \sin(\theta3) + E^2 \quad (3.6)$$

The equation 3.6 can be written in the following form by substituting the parameters C, D and E:

$$a \sin^2(\theta3) + b \sin(\theta3) + c = 0 \quad (3.7)$$

where:

$$a = 4z3^2(z1^2 - 2z1z2 \cos(\theta1 - \theta2) + z2^2)$$

$$b = 4z3(z2 \sin(\theta2) - z1 \sin(\theta1))(z1^2 - 2z1z2 \cos(\theta1 - \theta2) + z2^2 + z3^2 - z4^2)$$

$$c = (z1^2 - 2z1z2 \cos(\theta1 - \theta2) + z2^2 + z3^2 - z4^2)^2 - 4z3^2(z1^2 \cos^2(\theta1) - 2z1z2 \cos(\theta1) \cos(\theta2) + z2^2 \cos^2(\theta2))$$

Now, it is possible to obtain  $\theta3$  from the formula:

$$\theta3 = \sin^{-1} \left( \frac{-b \pm \sqrt{b^2 - 4ac}}{2a} \right) \quad (3.8)$$

When  $\theta3$  is known it is possible to calculate also  $\theta4$  from equation 3.3.

### Angular velocity analysis

The angular velocity analysis is conducted deriving the chain closure equation 3.1 in time, remembering that the driving crank moves with constant angular velocity.

$$\dot{\theta}4iz4e^{i\theta4} = \dot{\theta}2iz2e^{i\theta2} + \dot{\theta}3iz3e^{i\theta3} \quad (3.9)$$

Equation 3.9 is now separated into its real and imaginary parts:

$$\begin{cases} \dot{\theta}4z4 \sin(\theta4) = \dot{\theta}2z2 \sin(\theta2) + \dot{\theta}3z3 \sin(\theta3) & Real \\ \dot{\theta}4z4 \cos(\theta4) = \dot{\theta}2z2 \cos(\theta2) + \dot{\theta}3z3 \cos(\theta3) & Imaginary \end{cases} \quad (3.10)$$

From the imaginary component of equation 3.10,  $\dot{\theta}4$  can be obtained with the following formula:

$$\dot{\theta}4 = \frac{\dot{\theta}2z2 \cos(\theta2) + \dot{\theta}3z3 \cos(\theta3)}{z4 \cos(\theta4)} \quad (3.11)$$

Substituting  $\dot{\theta}4$  found in equation 3.11 into the real component of equation 3.10 it is possible to calculate also  $\dot{\theta}3$ , which results in:

$$\dot{\theta}3 = \frac{\dot{\theta}2z2(\sin(\theta2) - \cos(\theta2) \tan(\theta4))}{z3(\cos(\theta3) \tan(\theta4) - \sin(\theta3))} \quad (3.12)$$

Solving for the velocity  $\dot{\theta}3$  will allow the calculation of equation 3.11 to find  $\dot{\theta}4$ .

### Angular acceleration analysis

Deriving the equation 3.9 in time, it is possible to calculate the accelerations of the first kinematic chain:

$$z4 \left( \ddot{\theta}4i - \dot{\theta}4^2 \right) e^{i\theta4} = z2 \left( \ddot{\theta}2i - \dot{\theta}2^2 \right) e^{i\theta2} + z3 \left( \ddot{\theta}3i - \dot{\theta}3^2 \right) e^{i\theta3} \quad (3.13)$$

As done for the position and velocity analysis the equation 3.13 is divided into its real and imaginary components:

$$\begin{cases} z4 \left( \dot{\theta}4^2 \cos(\theta4) + \ddot{\theta}4 \sin(\theta4) \right) = z2 \left( \dot{\theta}2^2 \cos(\theta2) + \ddot{\theta}2 \sin(\theta2) \right) \\ \quad + z3 \left( \dot{\theta}3^2 \cos(\theta3) + \ddot{\theta}3 \sin(\theta3) \right) & Real \\ z4 \left( \ddot{\theta}4 \cos(\theta4) - \dot{\theta}4^2 \sin(\theta4) \right) = z2 \left( \ddot{\theta}2 \cos(\theta2) - \dot{\theta}2^2 \sin(\theta2) \right) \\ \quad + z3 \left( \ddot{\theta}3 \cos(\theta3) - \dot{\theta}3^2 \sin(\theta3) \right) & Imaginary \end{cases} \quad (3.14)$$

From the real component of equation 3.14 the angular acceleration  $\ddot{\theta}4$  can be found:

$$\ddot{\theta}4 = \frac{A + z3\ddot{\theta}3 \sin(\theta3)}{z4 \sin(\theta4)} \quad (3.15)$$

where  $A = z2 \left( \dot{\theta}2^2 \cos(\theta2) + \ddot{\theta}2 \sin(\theta2) \right) + z3\dot{\theta}3^2 \cos(\theta3) - z4\dot{\theta}4^2 \cos(\theta4)$  contains all the already known variables.

$\ddot{\theta}4$  can be calculated also from the imaginary component, in the form of:

$$\ddot{\theta}4 = \frac{B + z3\ddot{\theta}3 \cos(\theta3)}{z4 \cos(\theta4)} \quad (3.16)$$

where  $B = z2 \left( -\dot{\theta}2^2 \sin(\theta2) + \ddot{\theta}2 \cos(\theta2) \right) - z3\dot{\theta}3^2 \sin(\theta3) + z4\dot{\theta}4^2 \sin(\theta4)$  contains all the already known variables.

At this point 3.15 and 3.16 can be equaled solving for  $\ddot{\theta}3$ :

$$\ddot{\theta}3 = \frac{B \tan(\theta4) - A}{z3(\sin(\theta3) - \cos(\theta3) \tan(\theta4))} \quad (3.17)$$

When  $\ddot{\theta}3$  is known, it can be substituted in equation 3.15 or 3.16 and  $\ddot{\theta}4$  can be calculated as well.

### 3.2 Second kinematic chain - z1z2z5z6

In Figure 3.3 is represented the second kinematic chain of the mechanism that is to be studied.

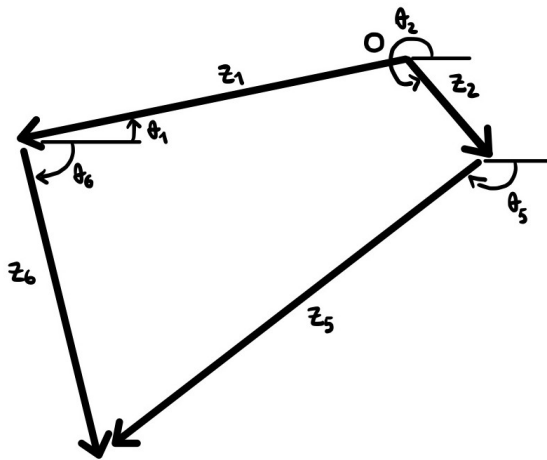


**Figure 3.3:** Second kinematic chain

The kinematic analysis of the second chain can be performed with the same operations done for the first chain, except the terms for links z4 and z3 are replaced with z6 and z5 respectively, therefore only the main results are reported.

## Angular position analysis

Below is reported the chain closure equation of the loop z1z2z5z6:

$$z1e^{i\theta 1} + z6e^{i\theta 6} = z2e^{i\theta 2} + z5e^{i\theta 5} \quad (3.18)$$

As done in Section 3.1, for the analysis of the position we go back to the shape of the equation:

$$a \sin^2(\theta_5) + b \sin(\theta_5) + c = 0 \quad (3.19)$$

where:

$$\begin{aligned}a &= 4z5^2(z2^2 - 2z1z2 \cos(\theta1 - \theta2) + z1^2) \\b &= 4z5(z2 \sin(\theta2) - z1 \sin(\theta1)) (z2^2 - 2z1z2 \cos(\theta1 - \theta2) + z1^2 + z5^2 - z6^2) \\c &= (z2^2 - 2z1z2 \cos(\theta1 - \theta2) + z1^2 + z5^2 - z6^2)^2 - 4z5^2(z2^2 \cos^2(\theta2) - 2z1z2 \cos(\theta1) \cos(\theta2) + z1^2 \cos^2(\theta1))\end{aligned}$$

From 3.19,  $\theta_5$  can be calculated using the inverse expression of sine:

$$\theta_5 = \sin^{-1} \left( \frac{-b \pm \sqrt{b^2 - 4ac}}{2a} \right) \quad (3.20)$$

Knowing  $\theta_5$ , with the following equation it is possible to calculate also  $\theta_6$ .

$$\theta_6 = \cos^{-1} \left( \frac{-z1 \cos(\theta1) + z2 \cos(\theta2) + z5 \cos(\theta5)}{z6} \right) \quad (3.21)$$

### Angular velocity analysis

Deriving equation 3.18 in time the angular velocity analysis of the chain z1z2z5z6 can be performed.

$$\dot{\theta}4iz4e^{i\theta4} = \dot{\theta}2iz2e^{i\theta2} + \dot{\theta}3iz3e^{i\theta3} \quad (3.22)$$

Separating equation 3.22 into its real and imaginary components, the velocities  $\dot{\theta}5$  and  $\dot{\theta}6$  can be found, in the form of the following equations.

$$\dot{\theta}6 = \frac{\dot{\theta}2z2 \cos(\theta2) + \dot{\theta}5z5 \cos(\theta5)}{z6 \cos(\theta6)} \quad (3.23)$$

$$\dot{\theta}5 = \frac{\dot{\theta}2z2(\sin(\theta2) - \cos(\theta2) \tan(\theta6))}{z3(\cos(\theta5) \tan(\theta6) - \sin(\theta5))} \quad (3.24)$$

### Angular acceleration analysis

With the following equations, the acceleration of the mobile links can be obtained.

$$z6 \left( \ddot{\theta}6i - \dot{\theta}6^2 \right) e^{i\theta6} = z2 \left( \ddot{\theta}2i - \dot{\theta}2^2 \right) e^{i\theta2} + z5 \left( \ddot{\theta}5i - \dot{\theta}5^2 \right) e^{i\theta5} \quad (3.25)$$

$$\ddot{\theta}6 = \frac{B + z5\ddot{\theta}5 \cos(\theta5)}{z6 \cos(\theta6)} \quad (3.26)$$

$$\ddot{\theta}5 = \frac{B \tan(\theta6) - A}{z5(\sin(\theta5) - \cos(\theta5) \tan(\theta6))} \quad (3.27)$$

where:

$$\begin{cases} A = z2 \left( \dot{\theta}2^2 \cos(\theta2) + \ddot{\theta}2 \sin(\theta2) \right) + z5\dot{\theta}5^2 \cos(\theta5) - z6\dot{\theta}6^2 \cos(\theta6) \\ B = z2 \left( -\dot{\theta}2^2 \sin(\theta2) + \ddot{\theta}2 \cos(\theta2) \right) - z5\dot{\theta}5^2 \sin(\theta5) + z6\dot{\theta}6^2 \sin(\theta6) \end{cases}$$

### 3.3 Third kinematic chain - z6z8z9z10

In Figure 3.4 is represented the third kinematic chain of the mechanism that is to be studied.

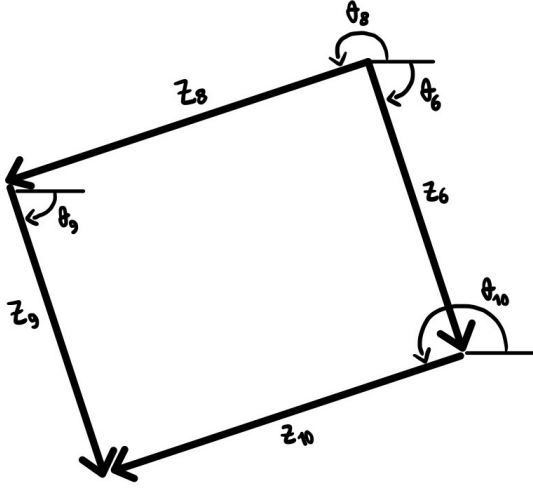


**Figure 3.4:** Third kinematic chain

The kinematic analysis of the third chain can be performed with the same operations done for the first chain, except the terms for links z1, z2, z3 and z4 are replaced with z8, z6, z10 and z9 respectively, therefore only the main results are reported.

#### Angular position analysis

Below is reported the chain closure equation of the loop z1z2z5z6:

$$z8e^{i\theta 8} + z9e^{i\theta 9} = z6e^{i\theta 6} + z10e^{i\theta 10} \quad (3.28)$$

With the following equation, the angles  $\theta 9$  and  $\theta 10$  can be derived:

$$a \sin^2(\theta 10) + b \sin(\theta 10) + c = 0 \quad (3.29)$$

where:

$$a = 4z10^2 (z6^2 - 2z8z6 \cos(\theta 8 - \theta 6) + z8^2)$$

$$b = 4z10(z6 \sin(\theta 6) - z8 \sin(\theta 8)) (z6^2 - 2z8z6 \cos(\theta 8 - \theta 6) + z8^2 + z10^2 - z9^2)$$

$$c = (z6^2 - 2z8z6 \cos(\theta 8 - \theta 6) + z8^2 + z10^2 - z9^2)^2 - 4z10^2 (z6^2 \cos^2(\theta 6) - 2z8z6 \cos(\theta 8) \cos(\theta 6) + z8^2 \cos^2(\theta 8))$$

From 3.29,  $\theta 10$  can be calculated:

$$\theta 10 = \sin^{-1} \left( \frac{-b \pm \sqrt{b^2 - 4ac}}{2a} \right) \quad (3.30)$$

Knowing  $\theta 5$ , with the following equation it is possible to calculate also  $\theta 6$ .

$$\theta 9 = \cos^{-1} \left( \frac{-z8 \cos(\theta 8) + z6 \cos(\theta 6) + z10 \cos(\theta 10)}{z9} \right) \quad (3.31)$$

### Angular velocity analysis

In this case, differently from the first two chains, all the links are mobile, so the derivation of 3.28 in time gives an expression of this type:

$$\dot{\theta}8iz8e^{i\theta8} + \dot{\theta}9iz9e^{i\theta9} = \dot{\theta}6iz6e^{i\theta6} + \dot{\theta}10iz10e^{i\theta10} \quad (3.32)$$

The equation 3.32 can be separated into its real and imaginary components and the velocities  $\dot{\theta}9$  and  $\dot{\theta}10$  can be obtained:

$$\dot{\theta}9 = \frac{\dot{\theta}6z6 \sin(\theta6) + \tan(\theta10)(\dot{\theta}8z8 \cos(\theta8) - \dot{\theta}6z6 \cos(\theta6)) - \dot{\theta}8z8 \sin(\theta8)}{z9(\sin(\theta10) - \tan(\theta10) \cos(\theta9))} \quad (3.33)$$

$$\dot{\theta}10 = \frac{\dot{\theta}8z8 \cos(\theta8) - \dot{\theta}6z6 \cos(\theta6) + \dot{\theta}9z9 \cos(\theta9)}{z10 \cos(\theta10)} \quad (3.34)$$

### Angular acceleration analysis

From the time derivative of 3.32 gives the equation describing the accelerations of the third kinematic chain.

$$z8 \left( \ddot{\theta}8i - \dot{\theta}8^2 \right) e^{i\theta8} + z9 \left( \ddot{\theta}9i - \dot{\theta}9^2 \right) e^{i\theta9} = z6 \left( \ddot{\theta}6i - \dot{\theta}6^2 \right) e^{i\theta6} + z10 \left( \ddot{\theta}10i - \dot{\theta}10^2 \right) e^{i\theta10} \quad (3.35)$$

From the real and imaginary components of 3.35 it is possible to calculate the accelerations  $\ddot{\theta}9$  and  $\ddot{\theta}10$ .

$$\ddot{\theta}9 = \frac{B + z10\dot{\theta}10 \cos(\theta10)}{z9 \cos(\theta9)} \quad (3.36)$$

$$\ddot{\theta}10 = \frac{B \tan(\theta9) - A}{z10(\sin(\theta10) - \cos(\theta10) \tan(\theta9))} \quad (3.37)$$

where:

$$\begin{cases} A = z6 \left( \dot{\theta}6^2 \cos(\theta6) + \ddot{\theta}6 \sin(\theta6) \right) + z10\dot{\theta}10^2 \cos(\theta10) - z8 \left( \dot{\theta}8^2 \cos(\theta8) + \ddot{\theta}8 \sin(\theta8) \right) - z9\dot{\theta}9^2 \cos(\theta9) \\ B = z6 \left( -\dot{\theta}6^2 \sin(\theta6) + \ddot{\theta}6 \cos(\theta6) \right) - z10\dot{\theta}10^2 \sin(\theta10) - z8 \left( -\dot{\theta}8^2 \sin(\theta8) + \ddot{\theta}8 \cos(\theta8) \right) + z9\dot{\theta}9^2 \sin(\theta9) \end{cases}$$

# Chapter 4

## Dynamic analysis

After performed the kinematic analysis the dynamic force analysis is usually done in order to determine the forces and torques in the system. It also returns all the joint forces of the leg mechanism. To perform the dynamic analysis, some assumptions need to be made:

1. The links are rigid
2. The friction in the joints are ignored
3. It is assumed that the operating crank of the leg mechanism will travel at constant velocity
4. The contact of the legs with the ground have no impact on the dynamic of the mechanism
5. There is no slip between the leg and the ground

When the foot is in contact with the ground there are too many unknowns than equations. According to the assumptions, different dynamic analyses can be carried out.

The free body diagram returns three equations for each link. There are two type of links used in the leg mechanism:

- binary link
- tertiary link

## Binary link

A free body diagram of a general binary link is shown in Figure 4.1

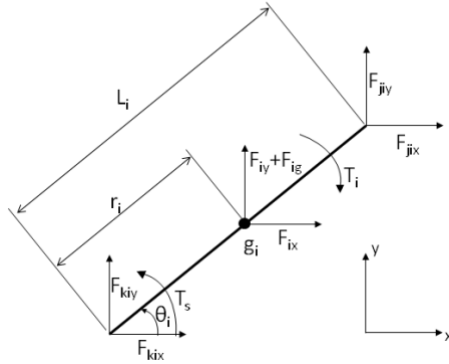


**Figure 4.1:** Free body diagram of a general binary link

By making the balance of forces, the sum of the x and y components of forces is equal to zero.

$$\begin{cases} \sum F_x = 0 = \sum_{j=1}^n F_{jix} + \sum_{k=1}^n F_{kix} + F_{ix} \\ \sum F_y = 0 = \sum_{j=1}^n F_{jiy} + \sum_{k=1}^n F_{kiy} + F_{iy} + F_{ig} \end{cases} \quad (4.1)$$

where the subscript  $i$  is the number of the link and  $k$  and  $j$  are the number of each link attached to the corresponding ends of the link.  $F_{ig}$  is the gravitational force of the mass of the link acting at the center of gravity, that is  $F_{ig} = m_i \cdot g$ , and  $F_i$  is the linear inertia forces acting at the center of gravity too. It is described as:  $F_i = -A_{gi} \cdot m_i e^{i\theta_{Ai}}$  where  $A_{gi}$  and  $\theta_{Ai}$  are the magnitude and direction of the acceleration at  $g_i$ .

In order to write the moment equilibrium equations we will use the following expression of the moment of a force  $F$  around a fulcrum:  $M_F = r_x F_y - r_y F_x$  which come from the determinant form of the vector cross product  $M_F = \vec{r} \times \vec{F}$  [19]. So, the summation of the moments about the center of gravity gives:

$$\sum M = 0 = T_i + T_s + \vec{r}_i \times \sum_{k_1}^{k_n} \vec{F}_{ki} + (L_i - \vec{r}_i) \times \sum_{j_1}^{j_n} \vec{F}_{ji} \quad (4.2)$$

rewriting the vector product of the forces in the cartesian form:

$$\sum M = 0 = T_i + T_s + r_i \sum_{k_1}^{k_n} [F_{kix} \sin \theta_i - F_{kiy} \cos \theta_i] + (L_i - r_i) \sum_{j_1}^{j_n} [-F_{jix} \sin \theta_i + F_{jiy} \cos \theta_i] \quad (4.3)$$

where  $r_i$  is the distance from one end of the link to the center of mass.  $T_s$  is the torque acted on the link from an attached shaft and  $T_i$  is the rotational inertia which is equal to the product of the inertia about the center of gravity and the angular acceleration of the link:  $T_i = -I_{gi} \cdot \alpha_i$ .

### Tertiary link

The second type of link found in the mechanism is the tertiary link which differs from the binary link in the particular position of the center of gravity. It can be calculated by taking the average of the x coordinates and the y coordinates of all the three vertices  $gi = \left( \frac{x_1+x_2+x_3}{3}, \frac{y_1+y_2+y_3}{3} \right)$ . The equations are then the same as the binary link with the only difference that the moments of the forces are calculated by the vectorial product of the forces and the distance from the vertices to the position of the centroid. In Figure 4.2 is reported a general free body diagram of a coupler.

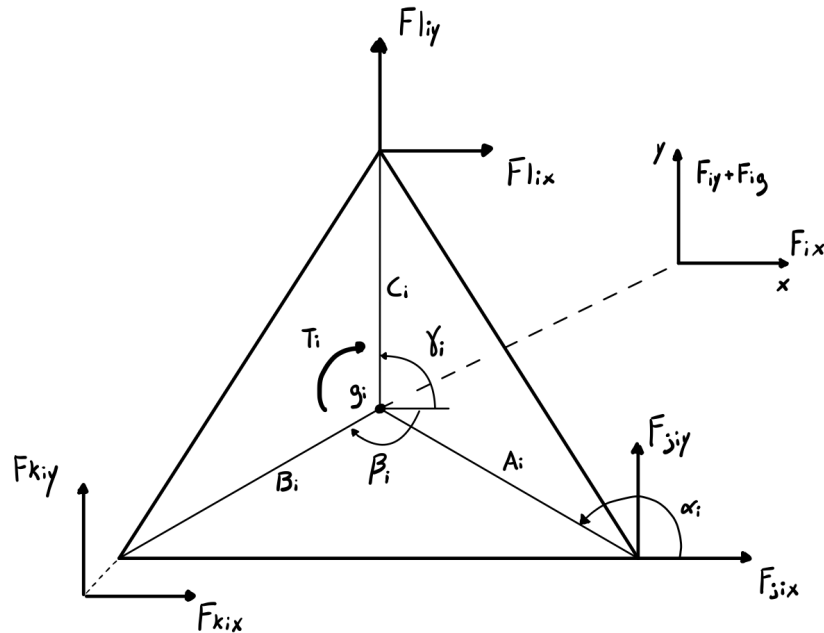


**Figure 4.2:** Free body diagram of the forces in a general triangular coupler

where  $A_i$ ,  $B_i$ ,  $C_i$  are the distance from the vertices to the centroid and  $\alpha$ ,  $\beta$  and  $\gamma$  are the respective angles.

## 4.1 Dynamics of link z2

In Figure 4.3 is reported the link z2.

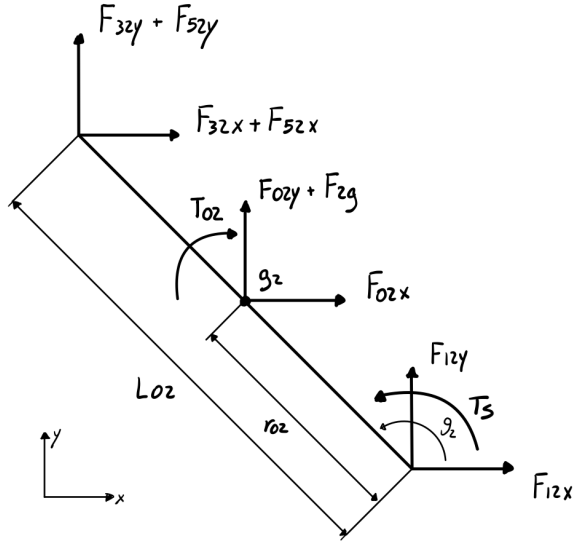


**Figure 4.3:** Free body diagram of the link z2

Summing the forces:

$$\sum F = 0 = \vec{F}_{02} + \vec{F}_{12} + \vec{F}_{32} + \vec{F}_{02} + \vec{F}_{52} + \vec{F}_{gy} \quad (4.4)$$

Separating into the x and y components with the known constants on the left, and remembering that  $F_{ij} = -F_{ji}$ :

$$\begin{cases} F_{02x} = -F_{12x} + F_{23x} + F_{25x} \\ F_{02y} + F_{2g} = -F_{12y} + F_{23y} + F_{25y} \end{cases} \quad (4.5)$$

For the moment equilibrium:

$$\sum M = 0 = T_{02} + r_{02} (F_{12x} \sin \theta_2 - F_{12y} \cos \theta_2) + (L_{02} - r_{02}) (-F_{32x} \sin \theta_2 + F_{32y} \cos \theta_2 - F_{52x} \sin \theta_2 + F_{52y} \cos \theta_2) + T_s \quad (4.6)$$

where  $T_s$  could be the torque applied to the mechanism in order to move the links which can be expressed by the ratio of power to angular velocity, and  $T_{02}$  is rotational inertia expressed as  $T_{02} = -I_{g2} \cdot \alpha_2$ .

## 4.2 Dynamics of link z3

In Figure 4.4 is reported the link z3.

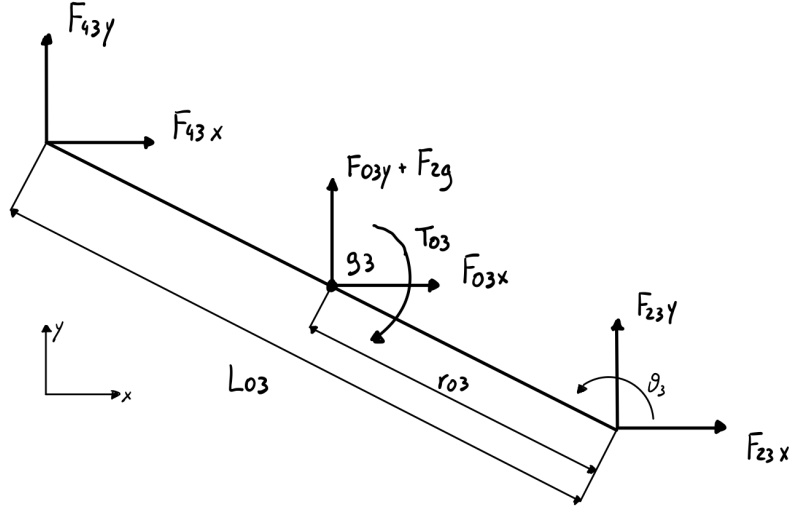


**Figure 4.4:** Free body diagram of the link z3

Summing the forces:

$$\sum F = 0 = \vec{F}_{03} + \vec{F}_{23} + \vec{F}_{43} + \vec{F}_{3g} \quad (4.7)$$

Separating into the x and y components with the known constants on the left:

$$\begin{cases} F_{03x} = -F_{23x} + F_{34x} \\ F_{03y} + F_{3gy} = -F_{23y} + F_{34y} \end{cases} \quad (4.8)$$

For the moment equilibrium:

$$\sum M = 0 = T_{03} + r_{03} (F_{23x} \sin \theta_3 - F_{23y} \cos \theta_3) + (L_{03} - r_{03}) (-F_{43x} \sin \theta_3 + F_{43y} \cos \theta_3) \quad (4.9)$$

where  $T_{03}$  is rotational inertia expressed as  $T_{03} = -I_{g3} \cdot \alpha_3$ .

### 4.3 Dynamics of coupling z4z7z8

In Figure 4.5 is reported the coupling z4z7z8.

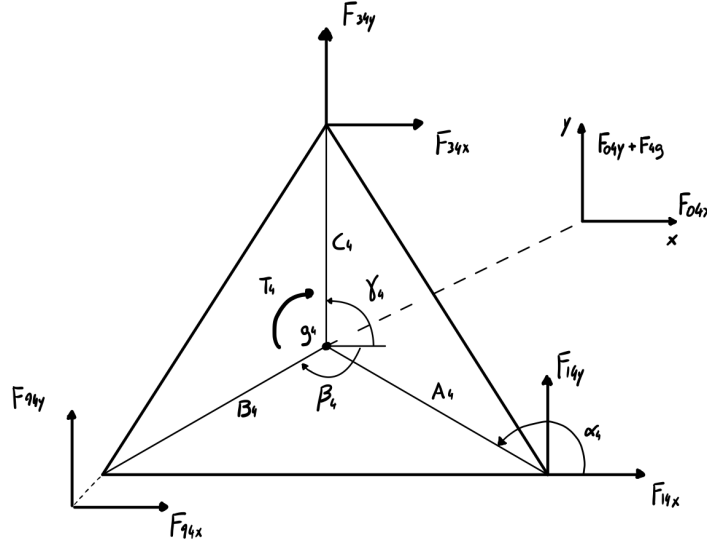


**Figure 4.5:** Free Body diagram of the coupling composed by the links z4z7z8

Summing the forces:

$$\sum F = 0 = \vec{F}_{04} + \vec{F}_{14} + \vec{F}_{34} + \vec{F}_{4g} \quad (4.10)$$

Separating into the x and y components with the known constants on the left:

$$\begin{cases} F_{04x} = -F_{14x} - F_{34x} + F_{49x} \\ F_{04y} + F_{4gy} = -F_{14y} - F_{34y} + F_{49y} \end{cases} \quad (4.11)$$

For the moment equilibrium:

$$\begin{aligned} \sum M = 0 = & T_{04} + r_{04} (F_{14x} \sin \alpha_4 - F_{14y} \cos \alpha_4) + C_4 (-F_{34x} \sin \gamma_4 + F_{34y} \cos \gamma_4) + \\ & + D_4 (-F_{94x} \sin \beta_4 + F_{94y} \cos \beta_4) \end{aligned} \quad (4.12)$$

where  $T_{04}$  is rotational inertia expressed as  $T_{04} = -I_{g4} \cdot \alpha_4$ .

#### 4.4 Dynamics of link z5

Figure 4.6 shows the link z5.

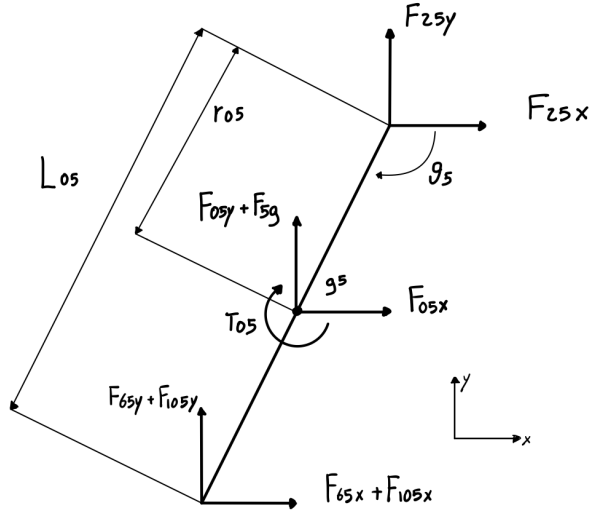


**Figure 4.6:** Free body diagram of the link z5

Summing the forces:

$$\sum F = 0 = \overrightarrow{F_{05}} + \overrightarrow{F_{25}} + \overrightarrow{F_{65}} + \overrightarrow{F_{105}} + \overrightarrow{F_5} \quad (4.13)$$

Separating into the x and y components with the known constants on the left:

$$\begin{cases} F_{05x} = -F_{25x} + F_{56x} + F_{510x} \\ F_{05y} + F_{5gy} = -F_{25y} + F_{56y} + F_{510y} \end{cases} \quad (4.14)$$

For the moment equilibrium:

$$\sum M = 0 = T_{05} + r_{05} (F_{25x} \sin \theta_5 - F_{25y} \cos \theta_5) + (L_{05} - r_{05}) (-F_{65x} \sin \theta_5 + F_{65y} \cos \theta_5 - F_{510x} \sin \theta_5 + F_{510y} \cos \theta_5) \quad (4.15)$$

where  $T_{05}$  is rotational inertia expressed as  $T_{05} = -I_{g5} \cdot \alpha_5$ .

## 4.5 Dynamics of link z6

Figure 4.7 shows the link z6.

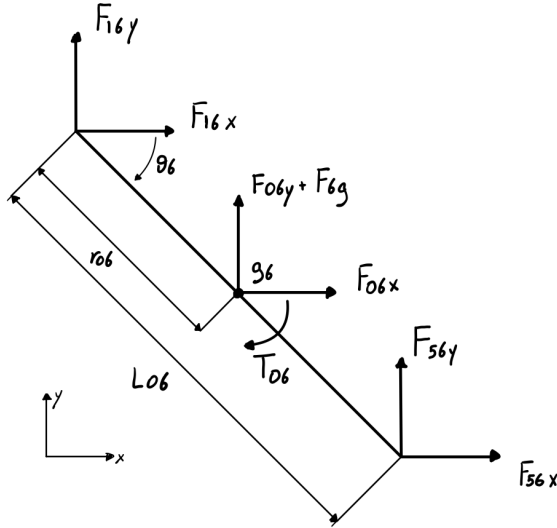


**Figure 4.7:** Free body diagram of the link z6

Summing the forces:

$$\sum F = 0 = \vec{F}_{06} + \vec{F}_{16} + \vec{F}_{56} + \vec{F}_{6g} \quad (4.16)$$

Separating into the x and y components with the known constants on the left:

$$\begin{cases} F_{06x} = -F_{16x} - F_{56x} \\ F_{06y} + F_{6gy} = -F_{16y} - F_{56y} \end{cases} \quad (4.17)$$

For the moment equilibrium:

$$\sum M = 0 = T_{06} + r_{06} (F_{16x} \sin \theta_6 - F_{16y} \cos \theta_6) + (L_{06} - r_{06}) (-F_{56x} \sin \theta_6 + F_{56y} \cos \theta_6) \quad (4.18)$$

where  $T_{06}$  is rotational inertia expressed as  $T_{06} = -I_{g6} \cdot \alpha_6$ .

## 4.6 Dynamics of link z9

Figure 4.8 shows the link z9.

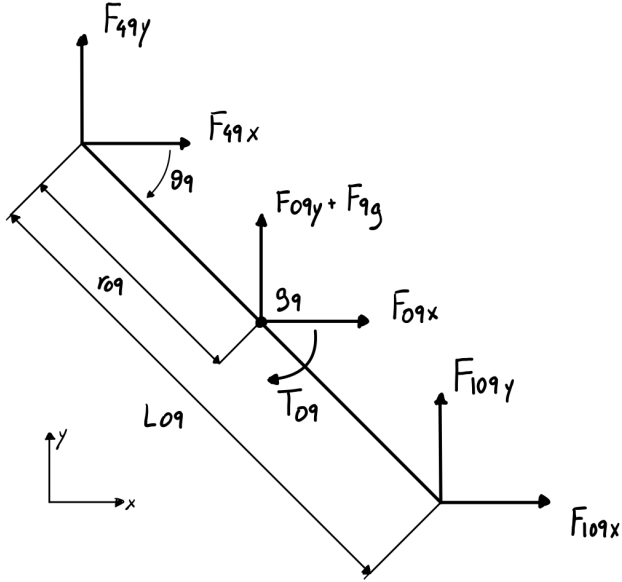


**Figure 4.8:** Free body diagram of the link z9

Summing the forces:

$$\sum F = 0 = \vec{F}_{09} + \vec{F}_{49} + \vec{F}_{109} + \vec{F}_{9g} \quad (4.19)$$

Separating into the x and y components with the known constants on the left:

$$\begin{cases} F_{09x} = -F_{49x} + F_{109x} \\ F_{09y} + F_{9gy} = -F_{49y} + F_{109y} \end{cases} \quad (4.20)$$

For the moment equilibrium:

$$\sum M = 0 = T_{09} + r_{09} (F_{49x} \sin \theta_9 - F_{49y} \cos \theta_9) + (L_{09} - r_{09}) (-F_{109x} \sin \theta_9 + F_{109y} \cos \theta_9) \quad (4.21)$$

where  $T_{09}$  is rotational inertia expressed as  $T_{09} = -I_{g9} \cdot \alpha_9$ .

## 4.7 Dynamics of coupling z10z11z12

In Figure 4.9 is reported the coupling z10z11z12.

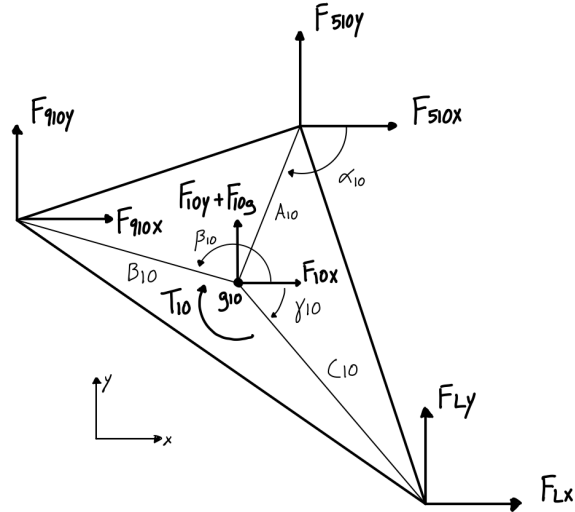


**Figure 4.9:** Free Body diagram of the coupling composed by the links z10z11z12

Summing the forces:

$$\sum F = 0 = \vec{F}_{10} + \vec{F}_{510} + \vec{F}_{910} + \vec{F}_L + \vec{F}_{10g} \quad (4.22)$$

Where  $F_L$  corresponds to the contact force of the mechanism with the ground which is usually known. Separating into the x and y components with the known constants on the left:

$$\begin{cases} F_{10x} + F_{Lx} = -F_{510x} - F_{910x} \\ F_{10y} + F_{10gy} + F_{Ly} = -F_{510y} - F_{910y} \end{cases} \quad (4.23)$$

For the moment equilibrium:

$$\begin{aligned} \sum M = 0 = & T_{10} + C_{10} (-F_{Lx} \sin \gamma_{10} + F_{Ly} \cos \gamma_{10}) + A_{10} (-F_{510x} \sin \alpha_{10} + F_{510y} \cos \alpha_{10}) + \\ & + D_{10} (-F_{910x} \sin \beta_{10} + F_{910y} \cos \beta_{10}) \end{aligned} \quad (4.24)$$

where  $T_{10}$  is rotational inertia expressed as  $T_{10} = -I_{g10} \cdot \alpha_{10}$ .

# Chapter 5

## Design example. Quadruped robot for obstacle avoidance

On 18 September 2019 an article titled *Walking Model of Jansen Mechanism-Based Quadruped Robot and Application to Obstacle Avoidance* was published online on Springer on behalf of the *Arabian Journal for Science and Engineering* ([4]). This article presents a four-legged quadruped robot-based upon Jansen mechanism developed by R. Singh and T.K. Bera, which is used for the application of obstacle avoidance. Being a legged robot it presents all the advantages over wheels machines stated in Section 1.1, particularly the agility on rough and irregular terrains.

In Figure 5.1a is presented the CAD model of the single leg where the connections between the links can be seen, while in Figure 5.1b is shown the path traced by various joints for both the CAD model and the prototype of the mechanism.

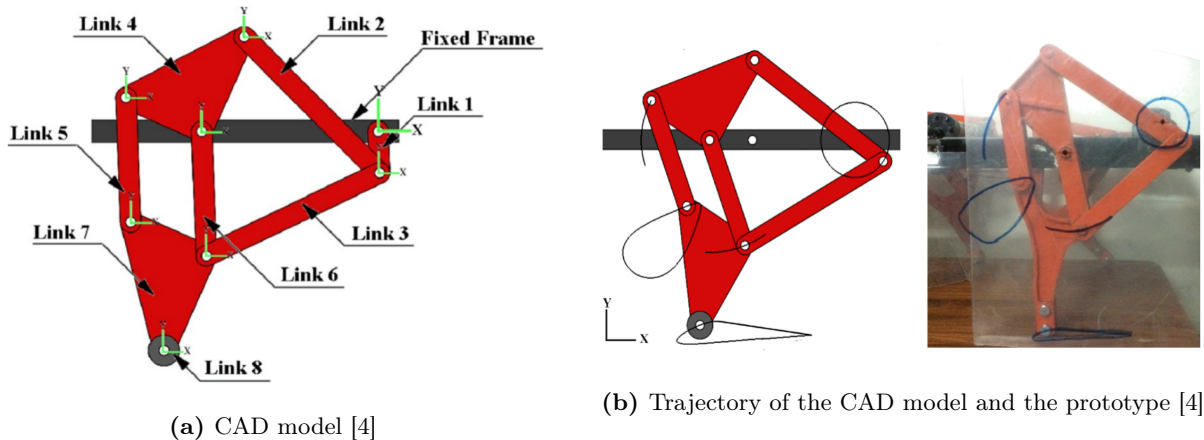


**Figure 5.1:** CAD model and trajectory followed by various joints

Link 8 is driven by an input torque which is given to link 1, therefore creating the motion of the leg. The whole mechanism is connected to the fixed frame that acts as chassis of the robot. The analytical model of the leg is based on the circle intersection method [9] from which the trajectory of any nodes can be determined in the reference frame. Building all the legs of the machine on the basis of the one shown in Figure 5.1 it was possible to develop the CAD model of the whole machine, shown in Figure 5.2.

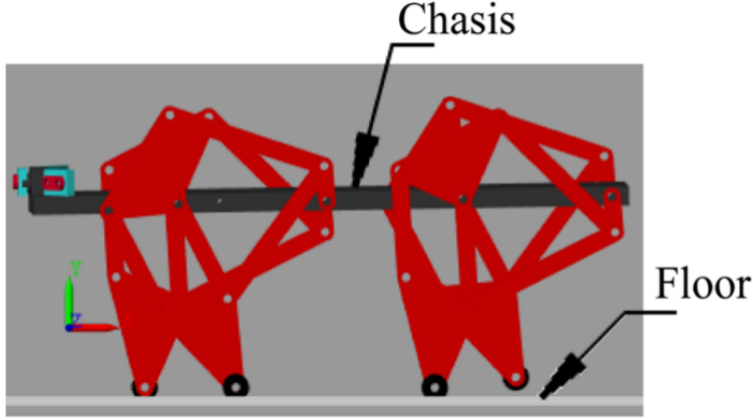


**Figure 5.2:** CAD model of the whole machine [4]

Figure 5.3, instead, presents the physical model (virtual prototype) of the single leg (5.3a) and the whole machine (5.3b) obtained using *Simscape™* toolbox within the *Simulink®* environment with the following link lengths:

$$\left\{ \begin{array}{l} \text{Link 1} \Rightarrow 0.05m \\ \text{Link 2} \Rightarrow 0.21m \\ \text{Link 3} \Rightarrow 0.18m \\ \text{Link 4 (tertiary link)} \Rightarrow [0.09 \ 0.11 \ 0.13]m \\ \text{Link 5} \Rightarrow 0.12m \\ \text{Link 6} \Rightarrow 0.12m \\ \text{Link 7 (tertiary link)} \Rightarrow [0.13 \ 0.11 \ 0.09]m \\ \text{Link 8} \Rightarrow \text{it is a stationary link} \end{array} \right.$$

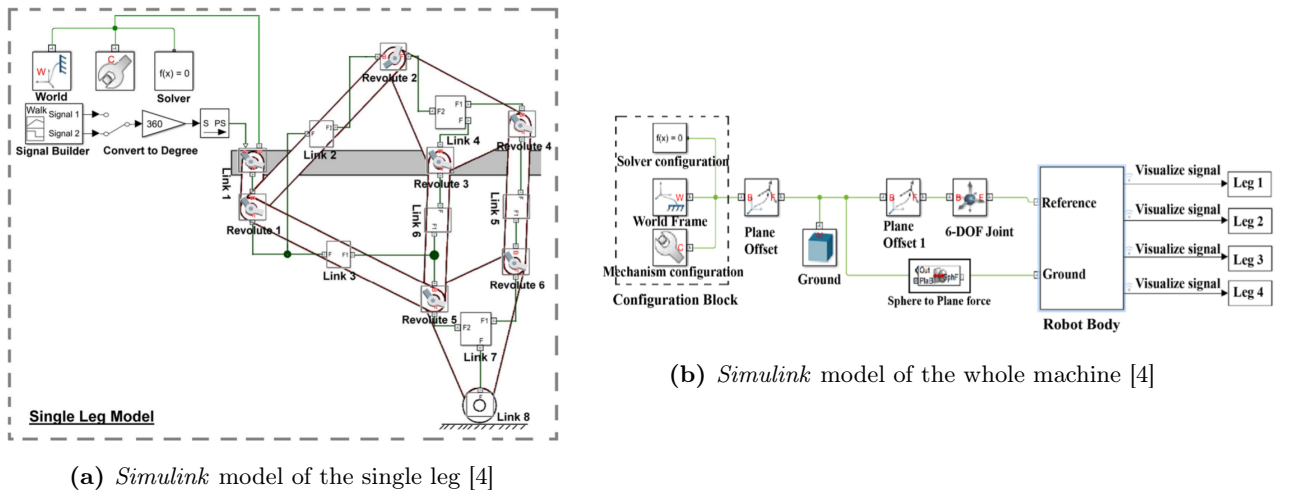


**Figure 5.3:** *Simulink* models

From Figure 5.3b it can be noticed that the ground is connected to the solver configuration, world frame and mechanism configuration blocks. The 6-DoF joint block which allows the robot to move

in three directions (X, Y and Z) and to rotate about axis X, Y and Z is connected to the robot model. The legs mechanisms are connected to the robot body. The sphere to plane force block is used to develop the friction model for ground surface where the foot of the robot acts as a sphere and the contact surface is considered as a plane in which the force is acting above and below it. To build the prototype of the robot Bera and Singh thought of making a square section chassis and used aluminium for the legs. To drive the mechanism, a drive torque is imparted to link 1 by four-ganged DC Johnson motors (60 rpm), powered by a 12V and 3A power supply, while the motion is controlled by an Arduino mega controller, which is directly connected to the laptop via USB cables. Obstacle detection and mapping of the surrounding environment is possible through the use of three ultrasonic HC-SR04 sensors that are mounted on the front part of the robot. The prototype model of the quadruped robot is shown in Figure 5.4 with a top view (5.4a) and a front view (5.4b).

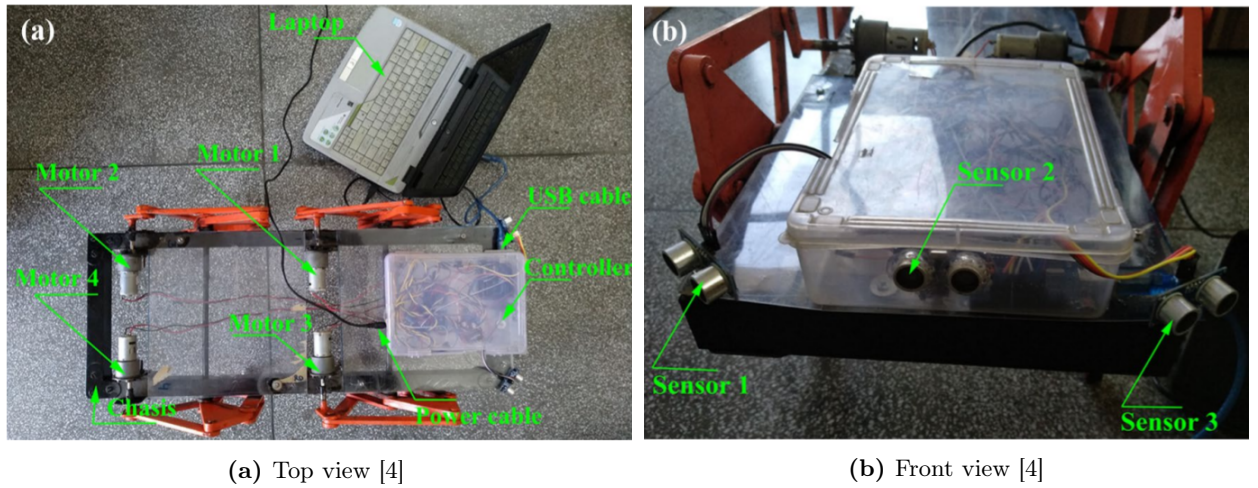


**Figure 5.4:** Prototype model of the robot [4]

The function of obstacle detection and avoidance is possible through the use of a fuzzy-based system which is shown in Figure 5.5.

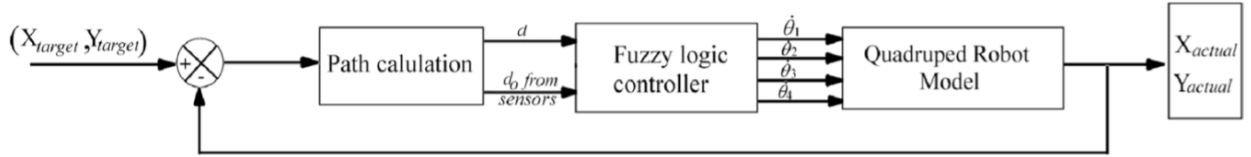


**Figure 5.5:** Fuzzy-based obstacle avoidance system [4]

The controller inputs are the distance from the target, whose position is known to the system, and the distance from the obstacles, computed by means of the ultrasonic sensors. The controller decides the angular motion of each motor shaft, the angular velocity of which represents the output. In Figure 5.6 the input functions of the controller can be seen.

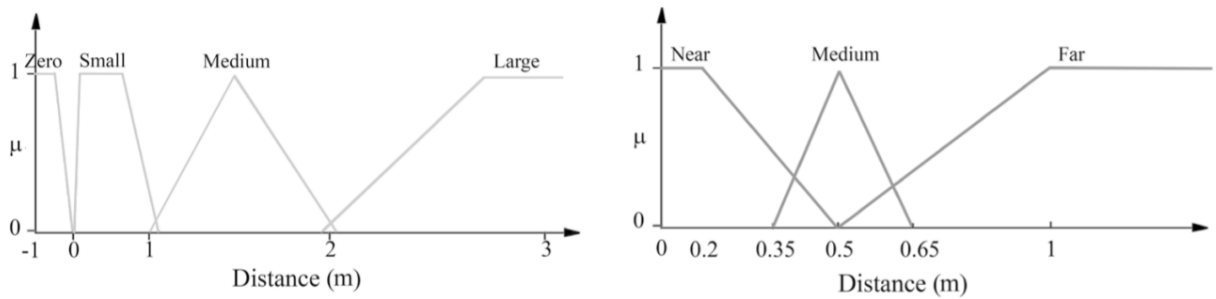


**Figure 5.6:** Distance of the robot from: the target (left), the obstacle (right) [4]

When the membership functions of a fuzzy controller have overlap, a smooth and continuous (i.e., no sudden change) control signal near the boundaries of the membership functions can be obtained.[4] As can be seen from Figure 5.6 there are overlapping for membership functions between Small and Medium, Large and Medium for robot's distance from the target and between Near and Medium, Far and Medium for robot's distance from the obstacle.

In Figure 5.7 the output function of the controller can be seen.

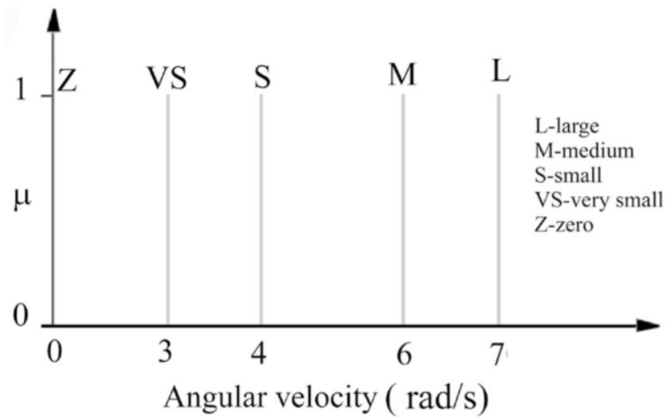


**Figure 5.7:** Output function of the controller: angular velocities of the motors [4]

To validate the fuzzy-based obstacle avoidance controller the robot was introduced in a closed boundary environment, shown in Figure 5.8, and has to reach the target without colliding with the walls of the boundary.

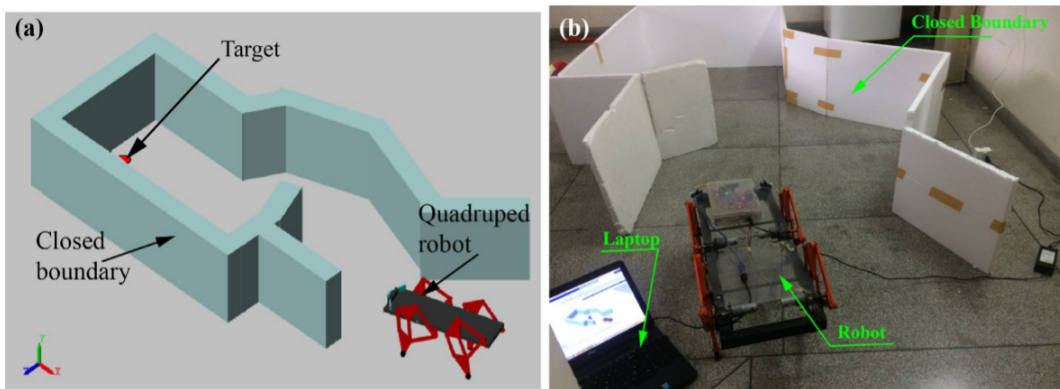


**Figure 5.8:** Setup for obstacle avoidance validation [4]

The results of the validation can be found in Figure 5.9, where the comparison of the simulation and experimental result of the path traced by the robot during obstacle avoidance in a closed boundary environment is shown.

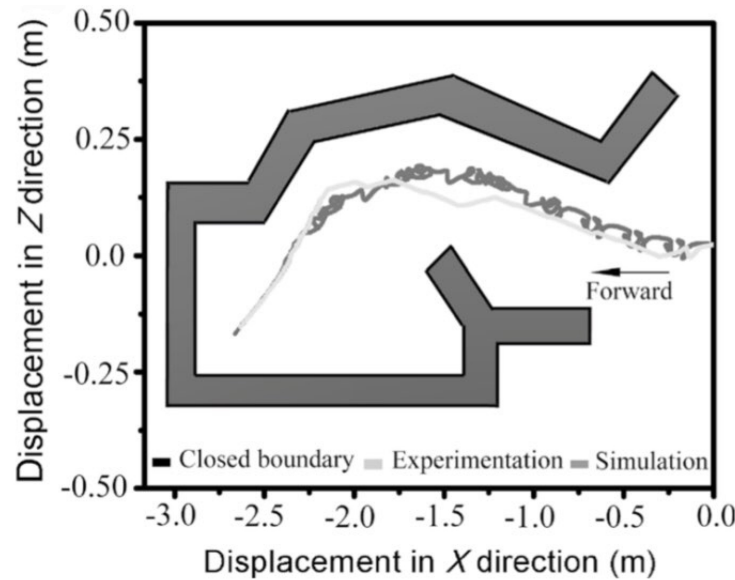


**Figure 5.9:** Results of the obstacle avoidance validation [4]

As can be seen from Figure 5.9 the path traveled by the robot in the simulation and in the experimentation are quite similar.

# **Chapter 6**

## **Conclusions**

In conclusion, it was possible to observe how, thanks to the use of linkages, it was possible to develop a new class of mechanisms capable of moving and avoiding obstacles. The report describes in broad term the historical background of the competing devices and outlines the limitations of the attempts to walk using a machine. Furthermore, it demonstrates how the Jansen's mechanism impact onto the studies of such walking machines. The details of the mechanism are discussed and developed in terms of kinematic and dynamic analysis. The best suited mechanism found in search is then described and demonstrated that a working prototype capable to detect and avoid obstacles was possible to been created.

# References

- [1] Daniel Giesbrecht. *Design and optimization of a one-degree-of-freedom eight-bar leg mechanism for a walking machine*. PhD thesis, The University of Manitoba, 2010.
- [2] Robert L. Norton. *Design of machinery : an introduction to the synthesis and analysis of mechanisms and machines*. McGraw-Hill series in mechanical engineering. Sixth edition, 2020.
- [3] Gim Soh and Nina Robson. Kinematic synthesis of minimally actuated multi-loop planar linkages with second order motion constraints for object grasping. ASME 2013 Dynamic Systems and Control Conference, DSCC 2013, 10 2013.
- [4] R Singh and TK Bera. Walking model of jansen mechanism-based quadruped robot and application to obstacle avoidance. *Arabian Journal for Science and Engineering*, 45(2):653–664, 2020.
- [5] Walking machines inc. steam man timeline. URL <http://cyberneticzoo.com/walking-machine-time-line/>.
- [6] D. J. Todd (auth.). *Walking Machines: An Introduction to Legged Robots*. Chapman and Hall Advanced Industrial Technology Series. Springer US, 1 edition, 1985.
- [7] Tesfaye Olana Terefe, Hirpa G Lemu, et al. Review and synthesis of a walking machine (robot) leg mechanism. 2019.
- [8] Leg mechanism. URL [https://en.wikipedia.org/wiki/Leg\\_mechanism](https://en.wikipedia.org/wiki/Leg_mechanism).
- [9] Anthony James Ingram. *A new type of mechanical walking machine*. PhD thesis, University of Johannesburg, 2006.
- [10] Chun-Yung Wang and June-Hao Hou. Analysis and applications of theo jansen's linkage mechanism-theo jansen's linkage mechanism on kinetic architecture. 2018.
- [11] Swadhin Patnaik. Analysis of theo jansen mechanism (strandbeest) and its comparative advantages over wheel based mine excavation system. *IOSR J Eng*, 5(7):43–52, 2015.
- [12] Strandbeest. URL <https://www.strandbeest.com/>.
- [13] U Kakati, M Rameez, PS Medhi, et al. Design and fabrication of a walking chair using linkage mechanism. *International Journal of Engineering Research & Technology (IJERT)*, 4(8), 2015.

- [14] Gopi Krishnan Regulan, Ganesan Kaliappan, and M Santhakumar. Development of an amphibian legged robot based on jansen mechanism for exploration tasks. In *Advancements in Automation, Robotics and Sensing*, pages 74–91. Springer Singapore, 2016.
- [15] Min-Chan Hwang, Feifei Liu, Jie Yang, and Yuanzhang Lin. The design and building of a hexapod robot with biomimetic legs. *Applied Sciences*, 9(14), 2019.
- [16] Neil Sclater. *Mechanisms and mechanical devices sourcebook*. McGraw-Hill Education, 2011.
- [17] S Sengupta and P Bhatia. Study of applications of jansen’s mechanism in robot. *Int J Adv Res Innov*, 5(3):354–357, 2017.
- [18] Kazuma Komoda and Hiroaki Wagatsuma. A proposal of the extended mechanism for the jansen linkage to modify the walking elliptic orbit and a study of cyclic base function. In *Proceedings of the 7th Annual Dynamic Walking Conference (DWC’12)*, 2012.
- [19] Arthur G Erdman and George N Sandor. *Mechanism design analysis and synthesis (Vol. 1)*. Prentice-Hall, Inc., 1997.
- [20] Manuel F. Silva and J.A. Tenreiro Machado. A historical perspective of legged robots. *Journal of Vibration and Control*, 13(9-10):1447–1486, 2007.
- [21] Vittore Cossalter, Mauro Da Lio, and Alberto Doria. *Meccanica applicata alle macchine*. Edizioni Progetto, 1999.